

A dynamic component model for forecasting high-dimensional realized covariance matrices[☆]

Luc Bauwens^{a,b,1}, Manuela Braione^{a,1}, Giuseppe Storti^{c,2,*}

^aUniversité catholique de Louvain, CORE, B-1348 Louvain-La-Neuve, Belgium

^bSKEMA Business School - Université de Lille

^cUniversità di Salerno, Department of Economics and Statistics, Fisciano, Italy

Abstract

The Multiplicative MIDAS Realized DCC (MMReDCC) model of [Bauwens et al. \(2016\)](#) simultaneously accounts for short and long-term dynamics in the conditional (co)volatilities of asset returns, in line with the empirical evidence suggesting that their level is changing over time as a function of economic conditions. This paper aims at improving the applicability of the model in two directions. First, by proposing an algorithm that relies on the maximization of an iteratively re-computed moment-based profile likelihood function, which mitigates the incidental parameter problem arising in large dimensions and keeps estimation feasible. Second, by illustrating a conditional bootstrap procedure to generate multi-step ahead predictions from the model. In an empirical application on a dataset of forty-six equities, the MMReDCC model is found to statistically outperform the selected benchmarks in terms of in-sample fit as well as in terms of out-of-sample covariance predictions. The latter are mostly significant in periods of high market volatility.

Keywords: Realized covariance, dynamic component models, multi-step forecasting, MIDAS, iterative algorithm.

1. Introduction

Building models for predicting the volatility of high dimensional portfolios is important in risk management and asset allocation. Previous developments on time-varying covariances in large dimensions include the constant conditional correlation (CCC) model of [Bollerslev \(1990\)](#), where the volatilities of each asset are allowed to vary through time but the correlations are time invariant, the RiskMetrics model by [Morgan \(1994\)](#), and the DECO model by [Engle and Kelly \(2012\)](#) who allow correlations to change over time and can be easily applied in vast dimensions. Recently, [Andersen et al. \(2001\)](#), [Barndorff-Nielsen and Shephard \(2001\)](#) and [Barndorff-Nielsen et al. \(2011\)](#), among others, opened up a new channel for increasing the precision of covariance matrix estimates and forecasts by exploiting the information of high frequency asset returns. This development has motivated several researchers to investigate models directly fitted to series of realized covariance matrices (see [Gouriéroux et al. \(2009\)](#), [Jin and Maheu \(2013\)](#) and [Chiriac and Voev \(2011\)](#), among others).

Despite the superiority of these models, illustrated for example by [Hautsch et al. \(2015\)](#), there still remain technical and practical challenges one needs to deal with when constructing covariance matrix forecasts for high-dimensional

[☆]The authors would like to thank Sébastien Laurent and Francesco Violante for providing the data used in the paper.

*Corresponding author

Email addresses: luc.bauwens@uclouvain.be (Luc Bauwens), manuela.braione@uclouvain.be (Manuela Braione), storti@unisa.it (Giuseppe Storti)

¹Luc Bauwens and Manuela Braione acknowledge support of the “Communauté française de Belgique” through contract “Projet d’Actions de Recherche Concertées 12/17-045”, granted by the “Académie universitaire Louvain”.

²Giuseppe Storti acknowledges funding from the Italian Ministry of Education, University and Research (MIUR) through PRIN project “Forecasting economic and financial time series: understanding the complexity and modeling structural change” (code 2010J3LZEN).

systems. First and foremost, the well-known “curse of dimensionality” problem, implying that the number of parameters grows as a power function of the cross-sectional model dimension. In order to save parameters, a simple solution is represented by the so called covariance (or correlation) targeting approach of Engle (2009), which consists in pre-estimating the constant intercept matrix in the model specification by linking it to the unconditional covariance matrix of returns. This method can be applied under the stationarity assumption of the model and is one of the most widely employed techniques to simplifying parameter estimation and reducing the computational burden when the numerical maximization of the likelihood function becomes difficult.

Recently, Bauwens et al. (2016) investigated a wide class of multivariate models that simultaneously account for short and long-term dynamics in the conditional (co)volatilities and correlations of asset returns, in line with the empirical evidence suggesting that their level is changing over time as a function of economic conditions (see, among others, Engle et al. (2013)). Herein we focus on the Multiplicative MIDAS Realized DCC (MMReDCC) model, whose main ingredients are a multiplicative component structure, a Mixed Data Sampling (MIDAS) filter to modeling the secular dynamics and a DCC-type parameterization for the short term component, directly inspired by the multivariate GARCH literature³. The extensive out-of-sample forecasting comparison performed by Bauwens et al. (2016), although not identifying a unique winner, shows that the MMReDCC model gives remarkably good performances in important financial applications such as Value-at-Risk forecasting and portfolio allocation. However, their results are limited to a relatively low dimensional setting (10 assets) and to a short-term forecasting horizon (1 day).

This paper extends the work by Bauwens et al. (2016) along these directions: estimation for high-dimensional systems and multi-step forecasting. We contribute to the first line of research by developing a computationally feasible procedure for the estimation of vast dimensional MMReDCC models. In this respect, it is important to remark that, although the introduction of a dynamic secular component in the structure of the model adds a major element of flexibility and enables to obtain more accurate forecasts than standard models reverting to constant mean levels (see Bauwens et al. (2016)), it also substantially increases the number of parameters to be estimated. Specifically, the long term component incorporates a scale intercept matrix with number of parameters equal to $n(n + 1)/2$, where n denotes the number of assets. In a vast dimensional framework, this quickly translates into the impossibility of estimating the model since the intercept matrix cannot be directly targeted.

Therefore, we propose to overcome this estimation issue by proposing an iterative procedure inspired by the covariance targeting idea of Engle (2009). More precisely, based on a Method of Moments estimator, we profile out the parameters of the intercept matrix and iteratively maximize the likelihood in terms of the other parameters of interest. We refer to this as the Iterative Moment-Based Profiling (IMP) estimator, as opposed to the Quasi Maximum Likelihood (QML) estimator which directly maximizes the likelihood with respect to the full parameter vector.

It is worth noticing that the proposed estimation procedure is inspired by a *switching algorithm* in the sense discussed by Boswijk (1995) and Cubadda et al. (2015) since the maximization of the overall likelihood is obtained by switching between optimizations over different blocks of parameters. This idea has a long standing tradition in the econometric analysis of time series. A simple, well known example of switching algorithm is given by the Cochrane-Orcutt iterative estimation procedure. Compared to conventional switching algorithms, the procedure that is here implemented incorporates an additional targeting step. In particular, it reduces the dimension of the optimization problem to be solved by concentrating out some of the parameters, the elements of the intercept matrix, by means of an iteratively re-computed moment-based estimator. A comprehensive simulation study is performed to assess the finite-sample properties of the proposed estimator which is found to deliver unbiased estimates and to be computationally reliable despite the large number of parameters involved.

The second contribution of the paper is the development of a resampling based procedure for the generation of multi-step ahead forecasts of the realized covariance matrices. The multiplicative component structure of the MMReDCC model makes the derivation of a closed-form expression for the h-step predictor impossible. Hence, to solve this issue we use a distribution-free procedure based on a residual bootstrap method. The bootstrap has been a standard tool for generating multi-step forecasts from non-linear and non-Gaussian time series models for more than two decades (see e.g. Clements and Smith (1997)). Its use has been later extended to univariate volatility modeling (see e.g. Pascual et al. (2006); Shephard and Sheppard (2010)). More recently, Fresoli and Ruiz (2015) have proposed

³We refer to Engle (2002) and Ghysels et al. (2007) as leading references for detailed discussions of the DCC model and MIDAS regressions.

a simple resampling algorithm that makes use of residual bootstrap to compute multi-step forecasts from DCC models. The bootstrap procedure which is implemented in this paper builds on the work of [Fresoli and Ruiz \(2015\)](#) but the algorithm is adapted to the dynamic modeling of realized covariance matrices.

Finally, the results of two different applications to real data are presented and discussed. In the first one, we focus on a low dimensional setting (ten assets), in which both the IMP and one-step QML estimation procedures are feasible, and compare the estimates obtained by means of both algorithms. We find that the IMP-based estimates are sufficiently close to the QML ones, so that using the IMP method in large dimensions is a sensible approach. We further consider the case in which the IMP estimated parameters are used as starting values for the one-step QMLE: despite an increase in the maximized likelihood value, the improvement can be considered rather marginal, thus suggesting that the implementation of the IMP algorithm alone may be sufficient in practical applications.

In the second application the MMReDCC model estimated for forty-six assets by the IMP method is used to generate forecasts of the realized covariance matrix up to twenty days ahead, and compared to existing benchmarks not accounting for short and long term (co)volatility dynamics. It emerges that over calm periods, simpler model specifications tend to be preferred especially at the shortest horizons, while during the 2007-2008 financial crisis accounting for time-varying long term dynamics in the conditional covariance process generates superior forecasts. The latter are particularly significant at the longest horizons.

The remainder of the paper is organized as follows. Section 2 briefly recalls the structure of the MMReDCC model and explains the curse of dimensionality issue. Section 3 introduces the IMP algorithm and Section 4 presents the results of a Monte Carlo experiment aimed at assessing the finite sample statistical properties of the proposed estimation algorithm. The bootstrap procedure for computing multi-step ahead forecasts is explained in Section 5, along with a simulation study to assess its final sample behavior. Section 6 contains the empirical results for the in-sample estimation comparison and the out-of-sample forecasting exercise. Section 7 concludes with some final remarks.

2. The MMReDCC model

Let C_t be a $n \times n$ positive definite and symmetric (PDS) realized estimator of the latent integrated covariance matrix of daily returns. In the following, unless otherwise stated, we will refer to C_t as the realized covariance (RC), although any other consistent PDS estimator could be used. Conditionally on the set consisting of all relevant information up to and including day $t - 1$, C_t is assumed to follow a n -dimensional central Wishart distribution:

$$C_t | I_{t-1} \sim W_n(\nu, S_t / \nu), \quad \forall t = 1, \dots, T, \quad (1)$$

where $\nu (> n - 1)$ is the degrees of freedom parameter and S_t is the PDS conditional mean matrix of order n . Under the assumption of absence of microstructure noise and other biases (see [Barndorff-Nielsen and Shephard \(2001\)](#)), S_t represents the conditional covariance matrix of returns, which is our object of interest.

In the MMReDCC model, S_t is designed to take into account the long run movements in the levels around which realized (co)variances (and by extension, correlations) fluctuate from day to day. To this extent, the model features a multiplicative decomposition of the conditional covariance matrix S_t into a smoothly varying or *secular* component $M_t = L_t L_t'$ and a short-lived component S_t^* , such that S_t can be rewritten as $S_t = L_t S_t^* L_t'$, where the matrix square root L_t can be obtained by a Cholesky factorization of M_t . These components can then be modeled separately.

First, the secular component is specified parametrically and extracted by means of a MIDAS filter assumed to be a weighted sum of K lagged realized covariance matrices over a long horizon, where the number of lags spanned in the MIDAS specification is usually chosen to minimize the trade-off between the highest in-sample likelihood value and the number of observations lost to initialize the filter. It is expressed as

$$M_t = \Lambda + \theta \sum_{k=1}^K \phi_k(\omega) C_{t-k}. \quad (2)$$

In the right hand side of Eq.(2), the first term Λ is a $n \times n$ symmetric and semi-positive definite matrix of constant pa-

Table 1: Number of parameters of MMRcDCC models

Note: Entries report the number of parameters as a function of the dimension n ; n_Λ denotes the number of unique parameters contained in the Λ matrix, ψ denotes the full vector of model parameters and $\tilde{\psi}$ the vector of parameters excluding n_Λ .

	$n = 5$	$n = 10$	$n = 20$	$n = 50$	$n = 100$
n_Λ	15	55	210	1275	5050
ψ	29	79	254	1379	5254
$\tilde{\psi}$	14	24	44	104	204

rameters, θ is a positive scalar and $\phi_k(\cdot)$ is a weight function parametrized according to the restricted Beta polynomial

$$\phi_k(\omega) = \frac{\left(1 - \frac{k}{K}\right)^{\omega-1}}{\sum_{j=1}^K \left(1 - \frac{j}{K}\right)^{\omega-1}}.$$

The scalar parameter ω determines the shape of the function and in order to achieve a time-decaying pattern of the weights, it is constrained to be larger than 1. For identification, the constraint $\sum_{k=1}^K \phi_k(\omega) = 1$ is imposed.

Second, the dynamics of the short term component S_t^* is specified according to a scalar DCC parametrization that enables a separate treatment of conditional volatilities and correlations, thus allowing for a high degree of flexibility. Letting X be any square matrix of arbitrary size n , in the remainder the notation $\text{diag}\{X\}$ is used to denote a $n \times n$ diagonal matrix with main diagonal elements equal to the corresponding diagonal elements of X . Therefore, assuming that $S_t^* = D_t^* R_t^* D_t^*$, where $D_t^* = \text{diag}\{S_t^*\}^{1/2}$, their scalar specifications correspond to the following equations:

$$S_{ii,t}^* = (1 - \gamma_i - \delta_i) + \gamma_i C_{ii,t-1}^* + \delta_i S_{ii,t-1}^*, \quad \forall i = 1, \dots, n \quad (3)$$

$$R_t^* = (1 - \alpha - \beta) I_n + \alpha P_{t-1}^* + \beta R_{t-1}^*, \quad (4)$$

where $\gamma_i > 0$, $\delta_i \geq 0$, $\gamma_i + \delta_i < 1$, $\alpha > 0$, $\beta \geq 0$, $\alpha + \beta < 1$, $C_t^* = L_t^{-1} C_t (L_t')^{-1}$ and $P_t^* = (\text{diag}\{C_t^*\})^{-1/2} C_t^* (\text{diag}\{C_t^*\})^{-1/2}$. The matrix C_t^* is the realized covariance matrix purged of its long term component and the matrix P_t^* is the corresponding short term realized correlation matrix. Mean reversion to unity in Eq.(4) and to an identity matrix in Eq.(4) is needed for identification of the different components. Let $\boldsymbol{\gamma} = \{\gamma_1, \dots, \gamma_n\}$, $\boldsymbol{\delta} = \{\delta_1, \dots, \delta_n\}$ for further use.

The parameters can be estimated by maximizing the following Wishart (quasi) log-likelihood function in one step:

$$\ell_T(\boldsymbol{\psi}) = -\frac{1}{2} \sum_{t=1}^T \left\{ \log |S_t(\boldsymbol{\psi})| + \text{tr}[S_t(\boldsymbol{\psi})^{-1} C_t] \right\}. \quad (5)$$

The finite-dimensional parameter vector⁴ $\boldsymbol{\psi} = \{\text{vech}(\Lambda), \theta, \omega, \boldsymbol{\gamma}, \boldsymbol{\delta}, \alpha, \beta\}$, has length $\{n_\Lambda + 2n + 4\}$ where $n_\Lambda = n(n+1)/2 \sim O(n^2)$ denotes the number of unique parameters included in the intercept matrix Λ of Eq.(2). It is obvious that, as n increases, the curse of dimensionality problem quickly arises, leading to the number of parameters listed in the first two rows of Table 1. Observe that estimation becomes already cumbersome after $n = 20$ and almost impossible for $n \geq 50$.

On the other hand, the last row of Table 1 shows that an obvious way to keep the model tractable is to avoid estimating the parameters of the matrix Λ . This would be sufficient to reduce the order to $2n + 4 \sim O(n)$, thus making the model estimable also for large n .

In the following section we put forward a feasible estimation procedure that aims at overcoming the direct estimation of the long term component intercept matrix, thus crucially mitigating the computational complexity of the model.

⁴Note that $\boldsymbol{\psi}$ does not include the degrees of freedom parameter ν , as the first order conditions for the estimation of the parameter vector $\boldsymbol{\psi}$ do not depend on ν (see Bauwens et al. (2016)).

3. An Iterative Moment based Profiling (IMP) algorithm

In this section we discuss an iterative procedure for fitting the MMReDCC model to large dimensional datasets. The basic idea underlying the proposed algorithm is to eliminate from the likelihood maximization the parameters of the intercept matrix Λ using a technique that builds upon the covariance targeting discussed in Pedersen and Rahbek (2014) for BEKK and Engle et al. (2008) for DCC models. First of all, notice that from Eq.(2) and the following relation

$$\Lambda = E(M_t) - \theta \sum_{k=1}^K \phi_k(\omega) E(C_{t-k}),$$

a moment based estimator of the Λ intercept matrix is given by

$$\hat{\Lambda} = \frac{1}{T} \sum_{t=1}^T \left[M_t - \theta \sum_{k=1}^K \phi_k(\omega) C_{t-k} \right]. \quad (6)$$

Obviously, given the latent nature of M_t , the estimator in Eq.(6) cannot be computed in practice and hence the covariance targeting approach cannot be applied in the usual way. It is worth noticing that, if L_t and S_t^* were assumed to be independent, given $E(S_t^*) = I_n$, it would hold that $E(C_t) = E(M_t)$, implying that an asymptotically equivalent version of Eq.(6) could be explicitly computed by replacing M_t by C_t . However, this is not the approach we pursue, since the assumption of independence of the short and long term sources is difficult to justify and would result in a rather counterintuitive and arbitrary constraint. Hence, we adopt a different method.

It can be seen from Eq.(6) that no estimate of Λ makes sense regardless of the value of (θ, ω) , so that by making this dependence explicit, it is possible to obtain an estimate of Λ as a function of (θ, ω) , i.e. $\hat{\Lambda}(\theta, \omega)$. In this way, a different estimate of Λ is required for each different value of the other two parameters. Therefore, by substituting $\hat{\Lambda}(\theta, \omega)$ for Λ in the Wishart QML function stated in Eq.(5), the following moment based QML approximation is obtained:

$$\tilde{\ell}_T(\tilde{\psi}) = -\frac{1}{2} \sum_{t=1}^T \left\{ \log |\tilde{L}_t(\theta, \omega) S_t^*(\tilde{\psi}) \tilde{L}'_t(\theta, \omega)| + \text{tr} \{ [\tilde{L}_t(\theta, \omega) S_t^*(\tilde{\psi}) \tilde{L}'_t(\theta, \omega)]^{-1} C_t \} \right\} \quad (7)$$

with $\tilde{\psi} = (\omega, \theta, \psi_{S^*})'$, $\psi'_{S^*} = (\gamma, \delta, \alpha, \beta)$ and

$$\tilde{M}_t(\theta, \omega) = \tilde{L}_t(\theta, \omega) \tilde{L}'_t(\theta, \omega) = \hat{\Lambda}(\theta, \omega) + \theta \sum_{k=1}^K \phi_k(\omega) C_{t-k}. \quad (8)$$

The method we propose consists in estimating the parameters in $\tilde{\psi}$ by a block-wise maximization of the moment-based QML function given in Eq.(7). First, conditional on some reasonable initial guess of (θ, ω) , $\tilde{\ell}_T(\tilde{\psi})$ is maximized with respect to the short term parameters ψ_{S^*} and then, conditional on $\hat{\psi}_{S^*}$, the same function is maximized with respect to (θ, ω) . The procedure is iterated for $j = 0, \dots, J$ until some convergence criterion on the likelihood is met.

To initialize the algorithm at $j = 0$, one can reasonably use as starting values the parameter estimates obtained by fitting the model to low dimensional subsets of data; also, an initial guess for the long term component $M_{t,0}$ could be either provided in a naive way, i.e. using the series of observed realized covariance matrices directly, or in a more sophisticated manner, by fitting to the data a nonparametric kernel smoother with an optimized bandwidth parameter. Note that in order to guarantee the positive definiteness of $\tilde{M}_t(\theta, \omega)$ in Eq.(8), it suffices to initialize $M_{t,0}$ from a PDS matrix and to impose $\theta > 0$. Given that the observed series of C_t , for every t , is PDS by definition, $\hat{\Lambda}(\theta, \omega)$ is assured to be at least semi-positive definite at each iteration $j > 0$.

Once $\Lambda_j(\theta_j, \omega_j)$ has been computed at the initial iteration $j = 0$, for every $j > 0$ the steps conducted in the algorithm are as follows:

Step 1 Plug $\Lambda_{j-1}(\theta_{j-1}, \omega_{j-1})$ into the dynamic equation for $\tilde{M}_{t,j}$ and $\tilde{L}_{t,j} = \text{chol}(\tilde{M}_{t,j})$ for all t ;

Step 2 For each asset $i = 1, \dots, n$, obtain the short term GARCH(1,1) parameters as follows:

$$\{\hat{\gamma}_{i,j}, \hat{\delta}_{i,j}\} = \arg \max_{\{\gamma_i, \delta_i\}} \tilde{\ell}_T(\theta_{j-1}, \omega_{j-1}, \alpha_{j-1}, \beta_{j-1});$$

Table 2: Simulation setting

In Panel A, for every $i = 1, \dots, n$ it holds $\{\gamma_i + \delta_i\} < 1$. Entries of Panel B are scalar parameters chosen to initialize the algorithm in both sets of simulation exercises.

PANEL A: PARAMETERS					
θ	0.5				
K	264				
ω	15				
Λ	$\Lambda_{i,i} = 0.02, \Lambda_{i,j} = 0.002$ for $i \neq j$				
γ_i	$\sim U(\gamma_0 - 0.02, \gamma_0 + 0.02), \gamma_0 = 0.2$				
δ_i	$\sim U(2\delta_0 + \gamma_i - 1 + 0.01, 1 - \gamma_i - 0.01), \delta_0 = 0.7$				
α	0.2				
β	0.7				
ν	$2n$				
T	1000, 2000				
burn-in observations	1000				
PANEL B: INITIAL VALUES					
θ_0	ω_0	$\gamma_{i,0}$	$\delta_{i,0}$	α_0	β_0
0.8	10	0.05	0.90	0.05	0.90

Step 3 Conditional on the estimated vectors $\hat{\boldsymbol{\gamma}}_j = (\hat{\gamma}_{1,j}, \dots, \hat{\gamma}_{n,j})'$ and $\hat{\boldsymbol{\delta}}_j = (\hat{\delta}_{1,j}, \dots, \hat{\delta}_{n,j})'$, maximize the same log-likelihood function with respect to the short term DCC correlation parameters:

$$\{\hat{\alpha}_j, \hat{\beta}_j\} = \arg \max_{\{\alpha, \beta\}} \tilde{\ell}_T(\theta_{j-1}, \omega_{j-1}, \hat{\boldsymbol{\gamma}}_j, \hat{\boldsymbol{\delta}}_j);$$

Step 4 Conditionally on the vector of short term parameter estimates $\hat{\boldsymbol{\psi}}_{S^*} = \{\hat{\boldsymbol{\gamma}}_j, \hat{\boldsymbol{\delta}}_j, \hat{\alpha}_j, \hat{\beta}_j\}$, maximize $\tilde{\ell}_T$ with respect to $\{\theta_j, \omega_j\}$; these estimates are used to compute an updated version of $\hat{\Lambda}_j(\theta_j, \omega_j)$;

Step 5 Check for convergence, *i.e.* if

$$\left| \frac{\tilde{\ell}_T(\tilde{\boldsymbol{\psi}}_j) - \tilde{\ell}_T(\tilde{\boldsymbol{\psi}}_{j-1})}{\tilde{\ell}_T(\tilde{\boldsymbol{\psi}}_{j-1})} \right| < \epsilon, \quad \epsilon = 0.000001;$$

if convergence is achieved, the algorithm stops; otherwise update all parameter estimates and go back to Step 1.

It is worth to stress that although $\tilde{\ell}_T(\tilde{\boldsymbol{\psi}})$ looks like a profile likelihood, it is not since $\hat{\Lambda}(\theta, \omega)$ is not a QML estimator but a feasible moment estimator. This motivates our choice to refer to Steps 1 – 5 as the Iterative Moment based Profiling algorithm, or IMP for short. This implies that $\tilde{\boldsymbol{\psi}}$ is typically less efficient than the standard QML estimator that maximizes Eq.(5) in one step. We come back to this issue in Section 6.1.

4. Simulation study

A Monte Carlo study is conducted to analyze the finite sample properties of the IMP estimator. We assume the MMRDCC to be the DGP and we generate 500 time series of lengths $T = 1000$ and 2000 for $n = 10, 20, 40$ and 50 , with true parameter values inspired by the estimates given in Bauwens et al. (2016), as summarized in Table 2.

It is important to stress that, in order to initialize the algorithm, parameter values have to be carefully chosen. This is a standard requirement in every optimization procedure where the initial amount of information on the model parameters is limited. In our situation we are mainly concerned with the impact that different choices of $M_{t,0}$, more than the remaining set of parameters, may have on the convergence of the IMP algorithm. We evaluate this by performing a robustness check based on the two possible initializations of $M_{t,0}$ mentioned in Section 3.

In the first set of repetitions $M_{t,0}$ is computed by fitting to the series of simulated realized covariance matrices a Nadaraya-Watson kernel estimator with a single bandwidth parameter for the whole covariance matrix. As in Bauwens et al. (2016) and Bauwens et al. (2013), the optimal bandwidth is selected by a least squares cross-validation criterion, where the six-month rolling covariance is used as the reference for the computation of least squares. In the second (equivalent) simulation study, $M_{t,0}$ is obtained by substituting in Eq. (6) the observed C_t for the latent matrix M_t at each t . In both cases, the initial scalar model parameters are set equal to the values listed in Panel B of Table 2. The

Table 3: **Simulation exercise I: summary statistics**

The table reports summary statistics of the first set of simulations where $M_{t,0}$ is initialized using a nonparametric kernel estimator, see Section 3. To save on space, $\bar{\gamma}$ and $\bar{\delta}$ are reported as averaged values across series and replications. RB denotes the Relative Bias computed over 500 replications. True parameter values used to simulate the process at the top of the table.

T= 1000							T= 2000						
	$\bar{\gamma}$	$\bar{\delta}$	α	β	θ	ω		$\bar{\gamma}$	$\bar{\delta}$	α	β	θ	ω_2
	0.197	0.705	0.2	0.7	0.5	15		0.197	0.705	0.2	0.7	0.5	15
n=10							n=10						
RB	0.098	-0.036	0.020	0.003	-0.058	-0.120	RB	-0.039	-0.002	0.033	0.003	0.053	-0.095
IQR	0.048	0.093	0.006	0.010	0.044	1.641	IQR	0.032	0.068	0.006	0.008	0.037	1.819
Mean	0.202	0.699	0.204	0.702	0.475	14.820	Mean	0.2	0.713	0.207	0.702	0.526	13.58
Min	0.176	0.660	0.191	0.679	0.393	7.460	Min	0.153	0.669	0.183	0.523	0.072	1.949
Max	0.214	0.735	0.220	0.728	0.709	18.943	Max	0.22	0.803	0.37	0.817	1.000	17.74
n=20							n=20						
RB	0.049	-0.009	0.019	0.001	-0.056	-0.110	RB	0.036	0.011	0.024	0.002	-0.014	-0.080
IQR	0.046	0.083	0.003	0.006	0.019	0.713	IQR	0.031	0.079	0.002	0.004	0.015	0.622
Mean	0.202	0.701	0.204	0.701	0.472	14.782	Mean	0.209	0.708	0.205	0.702	0.496	13.801
Min	0.171	0.633	0.197	0.687	0.430	12.802	Min	0.197	0.678	0.200	0.694	0.001	2.440
Max	0.219	0.744	0.211	0.711	0.532	16.759	Max	0.221	0.739	0.220	0.748	0.598	15.270
n=40							n=40						
RB	0.028	0.023	0.015	0.002	-0.049	-0.080	RB	0.033	0.029	0.022	0.002	-0.014	-0.072
IQR	0.042	0.077	0.002	0.002	0.011	0.372	IQR	0.030	0.064	0.001	0.002	0.007	0.263
Mean	0.208	0.715	0.203	0.701	0.476	14.810	Mean	0.209	0.719	0.204	0.702	0.493	13.925
Min	0.190	0.656	0.060	0.695	0.446	3.735	Min	0.181	0.671	0.182	0.674	0.172	1.000
Max	0.217	0.762	0.222	0.799	0.705	16.500	Max	0.221	0.761	0.223	0.744	0.837	14.760
n=50							n=50						
RB	0.027	0.011	0.016	0.001	-0.045	0.012	RB	0.029	0.027	0.017	0.001	-0.011	-0.037
IQR	0.042	0.076	0.001	0.002	0.008	0.293	IQR	0.030	0.056	0.001	0.002	0.007	0.220
Mean	0.208	0.716	0.203	0.701	0.473	15.182	Mean	0.208	0.720	0.203	0.701	0.494	14.442
Min	0.162	0.644	0.200	0.697	0.455	13.150	Min	0.191	0.657	0.199	0.695	0.474	12.089
Max	0.220	0.814	0.207	0.705	0.525	15.830	Max	0.222	0.763	0.207	0.707	0.529	16.238

estimation bias is evaluated by the relative bias (RB), computed as $\frac{1}{500} \sum_{i=1}^{500} \frac{\hat{\psi}_i - \psi}{\psi}$, along with the interquartile range (IQR), mean, minimum and maximum of the obtained parameter estimates. To save space, we report averaged bias results for the parameters of the MIDAS intercept matrix in a separate table.

Table 3 reports results from the first simulation exercise. As expected, the relative biases decrease as n or T increases. The biases for the parameters of the short term volatility and correlation components are very small, being smaller than five per cent in most of the cases, with one exception recorded for $\bar{\gamma}$ at $T = 1000$ for $n = 10$. As for the scalar parameters in the MIDAS specification, the bias for θ is negative in seven out of eight cases (the exception occurs for $n = 10$ at $T = 2000$) and ranging from the maximum of 5.8% (in absolute value) for $n = 10$ and $T = 1000$ to the lowest value of 1.1% for $n = 50$ and $T = 2000$. The bias on the ω parameter, also generally negative, tends to decrease with n but is usually of higher order (from 1.1 to 12% in absolute value). A similar behavior is observed for the IQR measure, which decreases across n and T but remains on higher values for the parameter ω . However, this does not represent a major concern as the Beta weight function is not very sensitive to small variations of this parameter and therefore we do not expect the likelihood function to be either.

Table 4 gives an idea of the robustness of the results to the other initialization of the long term component. Entries can be directly compared to those in Table 3. As hoped for, the initial choice has a minor impact on the overall accuracy of the estimator, as the parameter biases are in the same range of magnitude and the comments made earlier are still valid under this alternative scenario.

Figure 1 contains plots of the Monte Carlo standard deviations of the estimated θ , ω , α and β parameters against the cross-section size. In all cases, standard deviations tend to decline as the cross-section dimension grows, with a faster decline when $T = 2000$. The two approaches produce similar parameter standard deviations, with slightly bigger values recorded for θ and ω under the second simulation experiment in correspondence with the higher cross-section sizes.

If we move to analyzing the bias results for the scale MIDAS intercept matrix, Table 5 shows that under both sets of simulation exercises the estimator $\hat{\Lambda}(\theta, \omega)$ well approximates the true Λ matrix at all cross-section dimensions, with the parameter bias (averaged across diagonal and off-diagonal elements) clearly improving with increasing n and

Table 4: Simulation exercise II: summary statistics

The table reports summary statistics of the second set of simulations where $M_{t,0}$ is initialized from the series of realized covariance matrices, see Section 3. To save on space, $\bar{\gamma}$ and $\bar{\delta}$ are reported as averaged values across series and replications. RB denotes the Relative Bias computed over 500 replications. True parameter values used to simulate the process at the top of the table.

	T= 1000						T= 2000					
	$\bar{\gamma}$	$\bar{\delta}$	α	β	θ	ω	$\bar{\gamma}$	$\bar{\delta}$	α	β	θ	ω_2
	0.197	0.705	0.2	0.7	0.5	15	0.197	0.705	0.2	0.7	0.5	15
	n=10						n=10					
RB	-0.077	0.013	0.019	0.002	-0.032	-0.007	0.043	0.006	0.025	0.002	-0.012	-0.069
IQR	0.070	0.113	0.007	0.010	0.043	1.664	0.028	0.046	0.004	0.007	0.024	0.870
Mean	0.191	0.708	0.204	0.701	0.484	14.892	0.211	0.707	0.205	0.701	0.494	13.959
Min	0.107	0.588	0.191	0.678	0.393	6.678	0.189	0.654	0.196	0.686	0.435	9.614
Max	0.231	0.833	0.218	0.723	0.927	19.237	0.232	0.748	0.213	0.715	0.623	15.535
	n=20						n=20					
RB	0.048	-0.002	0.018	0.002	-0.045	-0.008	0.006	0.039	0.023	0.002	-0.011	-0.064
IQR	0.042	0.085	0.003	0.005	0.021	0.719	0.030	0.060	0.002	0.004	0.013	0.510
Mean	0.207	0.702	0.204	0.701	0.477	14.887	0.206	0.721	0.205	0.701	0.494	14.047
Min	0.196	0.649	0.197	0.689	0.429	6.751	0.164	0.680	0.199	0.692	0.467	11.108
Max	0.220	0.740	0.214	0.713	0.887	16.573	0.225	0.772	0.209	0.710	0.555	15.241
	n=40						n=40					
RB	0.046	0.017	0.017	0.003	-0.045	0.005	0.050	0.016	0.021	0.002	-0.012	-0.057
IQR	0.042	0.080	0.002	0.003	0.010	0.421	0.029	0.053	0.001	0.002	0.007	0.245
Mean	0.209	0.713	0.203	0.702	0.477	15.078	0.210	0.718	0.204	0.701	0.494	14.148
Min	0.197	0.682	0.193	0.696	0.116	6.895	0.194	0.658	0.202	0.697	0.479	8.433
Max	0.219	0.756	0.216	0.807	0.955	49.985	0.223	0.768	0.212	0.708	0.726	14.638
	n=50						n=50					
RB	0.029	0.028	0.016	0.002	-0.053	0.015	0.028	0.018	0.020	0.002	-0.017	-0.048
IQR	0.041	0.071	0.001	0.002	0.009	0.342	0.030	0.061	0.001	0.001	0.005	0.195
Mean	0.208	0.715	0.203	0.701	0.473	15.225	0.208	0.721	0.204	0.701	0.492	14.278
Min	0.190	0.632	0.200	0.698	0.457	14.190	0.184	0.674	0.202	0.698	0.437	11.178
Max	0.220	0.766	0.206	0.705	0.494	15.844	0.216	0.766	0.209	0.713	0.508	14.742

Table 5: Bias results for the scale MIDAS intercept matrix

Panel A reports summary statistics of the first simulation exercise where $M_{t,0}$ is initialized from a nonparametric smoother while Panel B reports results from the second simulation exercise where the series of observed realized covariance matrices are used. $RB_{(i,i)}$ denotes averaged values over diagonal terms, while $RB_{(i,j)}$ denotes averages over off diagonal terms. Number of simulations is 500.

PANEL A: SIMULATION EXERCISE I				PANEL B: SIMULATION EXERCISE II				
T=1000	T=2000		T=1000	T=2000		T=1000	T=2000	
n=10	n=10		n=10	n=10		n=10	n=10	
$RB_{(i,i)}$	0.080	$RB_{(i,i)}$	0.033	$RB_{(i,i)}$	0.075	$RB_{(i,i)}$	0.060	
$RB_{(i,j)}$	0.079	$RB_{(i,j)}$	0.000	$RB_{(i,j)}$	0.066	$RB_{(i,j)}$	0.040	
n=20	n=20		n=20	n=20		n=20	n=20	
$RB_{(i,i)}$	0.073	$RB_{(i,i)}$	0.068	$RB_{(i,i)}$	0.072	$RB_{(i,i)}$	0.058	
$RB_{(i,j)}$	0.062	$RB_{(i,j)}$	0.048	$RB_{(i,j)}$	0.060	$RB_{(i,j)}$	0.044	
n=40	n=40		n=40	n=40		n=40	n=40	
$RB_{(i,i)}$	0.073	$RB_{(i,i)}$	0.062	$RB_{(i,i)}$	0.073	$RB_{(i,i)}$	0.058	
$RB_{(i,j)}$	0.061	$RB_{(i,j)}$	0.046	$RB_{(i,j)}$	0.159	$RB_{(i,j)}$	0.043	
n=50	n=50		n=50	n=50		n=50	n=50	
$RB_{(i,i)}$	0.072	$RB_{(i,i)}$	0.004	$RB_{(i,i)}$	0.072	$RB_{(i,i)}$	0.058	
$RB_{(i,j)}$	0.057	$RB_{(i,j)}$	0.037	$RB_{(i,j)}$	0.058	$RB_{(i,j)}$	0.043	

T. Again, the direct comparison of Panels A and B confirms that the algorithm initialized from the series of realized covariance matrices overall performs no worse than the one initialized from a nonparametric smoother.

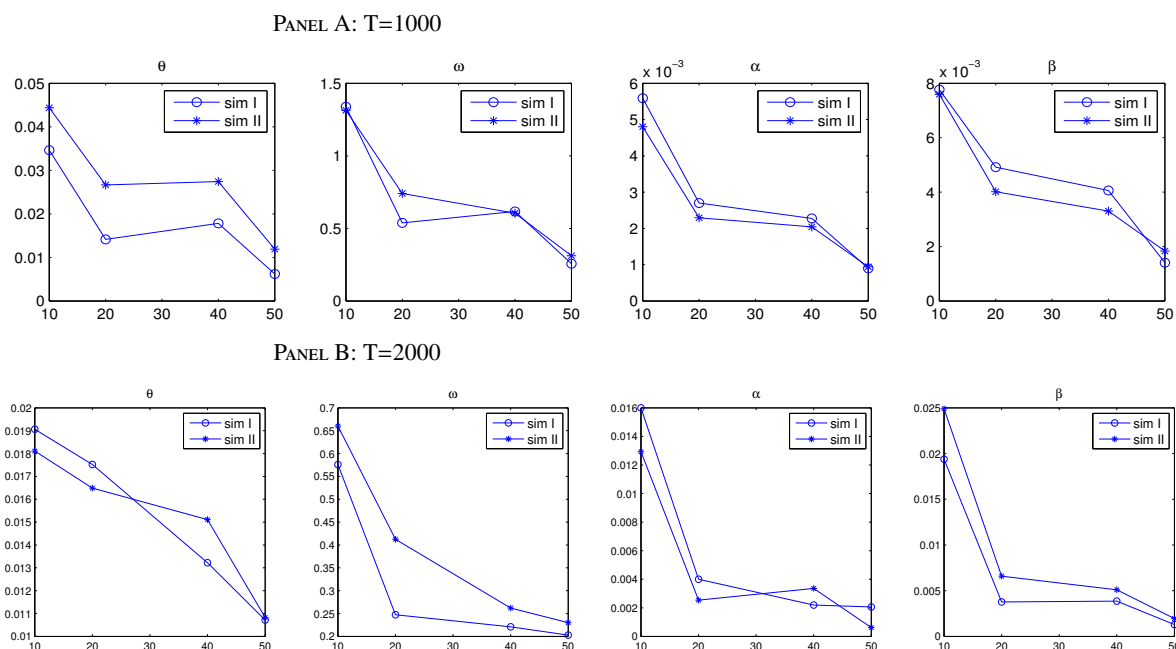
Finally, as the final interest is in the overall accuracy of the model in fitting conditional (co)variances and correlations (as a referee pointed out to us), we complement this section with an additional table that extends the Monte Carlo study to analyze the properties of the estimated in-sample series. Specifically, for each of the two exercises performed, we compare simulated and estimated variances, covariances and correlations in terms of mean, standard

deviation, lower and upper quartiles. Moreover, we compare the performance, in terms of variability, of the equally weighted portfolios constructed employing the true and the estimated conditional covariance matrix. Table 6 illustrates the strong similarity between the true series and the series obtained using the estimated model parameters, which supports the set of results discussed previously. Once again, no substantial difference can be detected between the two panels indexing the chosen initialization approach.

To summarize, the simulation study carried out in this section suggests that the proposed algorithm works accurately in finite samples and converges irrespective of the initialization choice made for the M_t matrices. Overall, the moment-based estimator used for iteratively targeting the constant intercept matrix in the secular component does not create a severe bias problem in the estimation of the other parameters, thus representing a feasible solution to alleviate the curse of dimensionality issue that would otherwise prevent the use of the MMReDCC model in high dimensional applications. Both initialization methods for $M_{t,0}$ can be used in practice. In the empirical section, we have opted for the nonparametric smoother.

Figure 1: IMP Monte Carlo standard deviations

The figure shows standard deviations of the IMP Monte Carlo estimated scalar parameters θ , ω , α and β against the cross-section dimension ranging from 10 to 50. Results from the first (Sim. I) and second (Sim. II) simulation study are jointly reported in Panel A for $T=1000$ and Panel B for $T=2000$.



5. Multi-step Forecasting

Models featuring short and long-run dynamics are particularly relevant for computing multi-step-ahead predictions, as their dynamic component structure is conceivably expected to be beneficial for long-term forecasts. Unfortunately, the complex nonlinear structure of the MMReDCC model prevents the analytical derivation of closed-form solutions. In order to overcome this limit, we compute multi-step predictions by means of a procedure based on bootstrap resampling. Subsection 5.1 formally introduces the procedure while the next one investigates its properties in finite samples.

5.1. A conditional bootstrap (CB) procedure

At the outset, notice that Eq.(1) implies that $E(C_t | \mathfrak{F}_{t-1}) = S_t$, so that C_t can be represented as

$$C_t = S_t^{1/2} U_t (S_t^{1/2})', \quad (9)$$

Table 6: Properties of the estimator

The table shows summary statistics of simulated (True) and estimated variance, covariance and correlation series, with values reported as averages across assets (n) and simulations (500). *Sim .I* denotes the first simulation exercise where $M_{t,0}$ is initialized from a nonparametric smoother while *Sim .II* uses the series of realized covariance matrices. In the last two columns we compare the properties of the volatilities of the n -dimensional equally weighted portfolios constructed using the true and the estimated conditional covariance matrix at each t . Q1 and Q3 respectively denote the first (0.25) and the third (0.75) quartile.

n	T	Stat.	Volatility (e-03)			Covariance (e-03)			Correlation			Portf. volatility			
			True	Sim .I	Sim .II	True	Sim .I	Sim .II	True	Sim .I	Sim .II	True	Sim .I	Sim .II	
10	1000	Mean	0.924	0.932	0.938	0.109	0.109	0.110	0.116	0.116	0.118	0.014	0.014	0.015	
		Std	0.217	0.220	0.230	0.148	0.149	0.147	0.149	0.148	0.145	0.002	0.002	0.001	
		Q1	0.765	0.771	0.757	0.010	0.010	0.011	0.011	0.012	0.012	0.013	0.013	0.014	
		Q3	1.050	1.060	1.059	0.203	0.204	0.205	0.223	0.222	0.243	0.015	0.015	0.016	
		2000	Mean	0.995	1.006	0.962	0.156	0.157	0.157	0.151	0.150	0.148	0.014	0.014	0.014
			Std	0.172	0.181	0.202	0.118	0.122	0.121	0.114	0.115	0.117	0.001	0.001	0.001
	Q1		0.836	0.840	0.827	0.060	0.059	0.058	0.062	0.060	0.061	0.014	0.014	0.013	
	20	1000	Mean	0.963	0.971	0.972	0.136	0.136	0.136	0.139	0.138	0.138	0.013	0.013	0.013
			Std	0.157	0.161	0.162	0.110	0.111	0.111	0.108	0.108	0.108	0.001	0.001	0.001
			Q1	0.828	0.833	0.832	0.055	0.055	0.055	0.060	0.060	0.060	0.013	0.013	0.013
			Q3	1.075	1.086	1.087	0.210	0.211	0.212	0.218	0.218	0.218	0.014	0.014	0.014
			2000	Mean	0.963	0.973	1.002	0.136	0.137	0.157	0.139	0.138	0.152	0.013	0.013
Std				0.161	0.168	0.158	0.113	0.115	0.107	0.111	0.111	0.101	0.001	0.001	0.001
Q1		0.828		0.832	0.854	0.055	0.055	0.072	0.060	0.059	0.075	0.013	0.013	0.013	
40		1000	Mean	1.040	1.048	1.294	0.188	0.189	0.235	0.176	0.175	0.178	0.014	0.015	0.015
			Std	0.123	0.131	0.805	0.087	0.088	0.215	0.079	0.079	0.076	0.001	0.001	0.001
			Q1	0.894	0.896	0.902	0.102	0.103	0.106	0.106	0.106	0.109	0.014	0.014	0.014
			Q3	1.168	1.181	1.285	0.262	0.264	0.288	0.245	0.244	0.248	0.015	0.015	0.015
			2000	Mean	1.046	1.042	1.059	0.191	0.198	0.195	0.178	0.179	0.179	0.015	0.015
	Std			0.123	0.125	0.129	0.088	0.089	0.088	0.078	0.078	0.078	0.001	0.001	0.001
	Q1	0.899		0.876	0.905	0.106	0.109	0.107	0.109	0.109	0.110	0.014	0.014	0.014	
	50	1000	Mean	1.078	1.086	1.098	0.212	0.213	0.221	0.191	0.190	0.195	0.015	0.015	0.015
			Std	0.115	0.123	0.120	0.082	0.082	0.080	0.071	0.071	0.068	0.001	0.001	0.001
			Q1	0.918	0.920	0.928	0.118	0.118	0.124	0.119	0.119	0.124	0.015	0.015	0.015
			Q3	1.222	1.234	1.249	0.294	0.296	0.304	0.262	0.261	0.266	0.016	0.016	0.016
			2000	Mean	1.088	1.098	1.088	0.219	0.220	0.214	0.195	0.195	0.191	0.015	0.015
Std				0.114	0.121	0.123	0.082	0.083	0.084	0.070	0.070	0.072	0.001	0.001	0.001
Q1		0.925		0.928	0.922	0.123	0.123	0.119	0.124	0.123	0.120	0.015	0.015	0.015	
2000		Q3	1.235	1.249	1.235	0.302	0.304	0.295	0.266	0.265	0.261	0.016	0.016	0.016	

where U_t is an element of a sequence of iid random matrices with $E(U_t) = I_n$, and $S_t^{1/2}$ is any PDS matrix such that $S_t^{1/2}(S_t^{1/2})' = S_t$. If $U_t \sim W_n(\nu, I_n/\nu)$, the Wishart assumption of Eq.(1) is recovered, but this is not needed to justify the bootstrap procedure used for generating multi-step-ahead forecasts of the realized covariance matrix C_t . The procedure is described in the following six steps.

Step 1 Estimate the model on $\{C_t, t = 1, \dots, T\}$ and obtain the parameter vector $\hat{\psi} = \{\text{vech}(\hat{\Lambda}), \hat{\theta}, \hat{\omega}, \hat{\gamma}, \hat{\delta}, \hat{\alpha}, \hat{\beta}\}$ to compute the estimated conditional covariance \hat{S}_t .

Step 2 Compute the estimated residuals

$$\hat{U}_t = \hat{S}_t^{-1/2} C_t (\hat{S}_t^{-1/2})', \quad t = 1, \dots, T$$

and rescale them to enforce their sample mean to be equal to I_n :

$$\tilde{U}_t = (\hat{E}_u^{-1/2}) \hat{U}_t (\hat{E}_u^{-1/2})',$$

where $\hat{E}_u = (1/T) \sum_{t=1}^T \hat{U}_t$. The rescaled \tilde{U}_t can then be used to generate bootstrap replicates of C_{T+j} , for $j = 1, \dots, h$, where h denotes the chosen forecast horizon.

Step 3 Draw with replacement a bootstrap sample $\{\tilde{U}_{T+1|T}, \dots, \tilde{U}_{T+h|T}\}$ of length h from the empirical CDF of $\{\tilde{U}_t, t = 1, \dots, T\}$.

Step 4 Initialize the procedure at $C_T, \hat{R}_T^*, \hat{P}_T^*, \hat{S}_T^*$ and \hat{L}_T . For $j = 1, \dots, h$, recursively generate a sequence of bootstrap

replicates of C_{T+j} as follows:

$$\begin{aligned}
R_{T+j|T}^* &= (1 - \hat{\alpha} - \hat{\beta})I_n + \hat{\alpha}P_{T+j-1|T}^* + \hat{\beta}R_{T+j-1|T}^*, \\
S_{ii,T+j|T}^* &= (1 - \hat{\gamma}_i - \hat{\delta}_i) + \hat{\gamma}_i C_{ii,T+j-1|T}^* + \hat{\delta}_i S_{ii,T+j-1|T}^*, \\
S_{T+j|T}^* &= (\text{diag}\{S_{T+j|T}^*\})^{1/2} R_{T+j|T}^* (\text{diag}\{S_{T+j|T}^*\})^{1/2}, \\
S_{T+j|T} &= L_{T+j|T} S_{T+j|T}^* L'_{T+j|T}, \\
C_{T+j|T} &= S_{T+j|T}^{1/2} \tilde{U}_{T+j|T} (S_{T+j|T}^{1/2})', \\
M_{T+j|T} &= \hat{\Lambda}(\theta, \omega) + \hat{\theta} \sum_{k=1}^K \phi_k(\hat{\omega}) C_{T-k+j|T}, \\
L_{T+j|T} &= M_{T+j|T}^{1/2}, \\
C_{T+j|T}^* &= L_{T+j|T}^{-1} C_{T+j|T} (L'_{T+j|T})^{-1}, \\
P_{T+j|T}^* &= (\text{diag}\{C_{T+j|T}^*\})^{-1/2} C_{T+j|T}^* (\text{diag}\{C_{T+j|T}^*\})^{-1/2}.
\end{aligned}$$

Step 5 Repeat steps 3–4 B times, where B is set sufficiently large (e.g. $B=5000$). As a result, the procedure generates an array of $h \times B$ bootstrap replicates $(C_{T+j|T}^{(1)}, \dots, C_{T+j|T}^{(B)})$ for $C_{T+j|T}$.

Step 6 Finally, the h -steps-ahead forecast is obtained as

$$\hat{S}_{T,h} = \frac{1}{B} \sum_{b=1}^B C_{T+h|T}^{(b)}.$$

It is worth to mention that the proposed procedure is applied by conditioning on the estimated model parameters, namely by keeping fixed the parameter estimates in all bootstrap forecasts of C_{T+j} , for $j = 1, \dots, h$, such that the achieved bootstrap h -steps ahead prediction depends only on the resampled residuals. Clearly, this could be relaxed in order to account for the variability associated to parameter estimation by re-estimating ψ on each bootstrap replicate, but it would come at the not negligible cost of increasing computational complexity and time. Overall, the results presented in Section 5.2 provide sufficient evidence that our approach works fine in finite samples.

Finally, even if our primary interest is in forecasting from MMReDCC models, the proposed forecasting procedure is very general and can be readily adapted to any model that admits the representation in Eq.(9), where S_t is modeled as a function of past information \mathfrak{F}_{t-1} . For example, in the empirical application which is presented in Section 6.2, we also use it to generate multi-step ahead forecasts of C_t from the cRDCC model of Bauwens et al. (2012). To this purpose, the dynamic equations in step 4 must be replaced by those pertaining to the specific model of interest.

5.2. Finite sample properties

In order to analyze the finite sample behavior of the proposed bootstrap procedure, we devise a simple Monte Carlo experiment. Namely, we generate 1000 series with the MMReDCC model using the same simulation design used in Section 4, with the nonparametric smoother chosen as the initialization method for $M_{t,0}$ ⁵. The sample sizes considered are $T = 1000$ and 2000 and the cross-sectional dimensions are $n = 5, 10, 20$ and 50 . In each case, we generate $j = 1, \dots, h$ future values of the simulated series, where $h = 2, 10$ and 20 , that are considered as the reference forecasting sample.

For each obtained set of B bootstrap replicates $(C_{T+j|T}^{(1)}, \dots, C_{T+j|T}^{(B)})$, we compute the corresponding prediction limits, defined as the quantiles of the bootstrap distribution function of $C_{T+j|T}^{(b)}$ ($b = 1, \dots, B$). More specifically, if $D_{C,B}(z)$ is an estimate of the distribution function $D_C(z) = Pr(C_{T+j|T} \leq z)$, then, a $100(1 - \vartheta)\%$ prediction interval for C_{T+j} is achieved as

$$[L_{C,B}(z), U_{C,B}(z)] = \left[Q_{C,B} \left(\frac{\vartheta}{2} \right), Q_{C,B} \left(1 - \frac{\vartheta}{2} \right) \right], \quad (10)$$

⁵Results obtained employing the alternative initialization approach are qualitatively similar and thus not reported for brevity.

with $Q_{C,B} = D_{c,B}^{-1}$. Bootstrap intervals are constructed based on $B=999$ replicates with nominal coverages $1 - \vartheta$ equal to 0.90, 0.95 and 0.99. After this, we compute the empirical coverage by counting the number of future values inside the corresponding intervals as $(1 - \vartheta)^* = \{L_{C,B} \leq C_{T+j} \leq U_{C,B}\}$. In addition we compute left and right coverage as the proportion of predictions falling below $L_{C,B}$ and above $U_{C,B}$, respectively.

Results are reported in Table 7 as averages across univariate variance (left panel) and covariance (right panel) series. First of all, we can notice that results are qualitatively similar across the two panels. It emerges that the intervals for future volatilities and covolatilities at multiple-steps ahead have average coverages close to the nominal values, and that their performance improves as the sample size increases from 1000 to 2000 observations.

The table also shows that the coverage rates depend on the forecast horizon, and that they have a tendency to decrease as horizons increase. This comes as a consequence of the parameter estimation variability that is not accounted for, as well as from the addition of error uncertainty. However, even if for $h > 2$ there is a slight undercoverage, coverage values are never below their nominal levels by more than 2.7%, and this happens irrespective of the forecast horizon or the considered sample size.

Overall, Monte Carlo results show that the proposed bootstrap procedure is capable of generating accurate point and interval forecasts from the MMReDCC model.

6. Empirical Applications

This section contains two empirical applications. The first application provides the estimation results for the IMP estimator in comparison with the standard QML estimator in the ideal case where both can be computed. The second one is performed in a large dimensional system and aims at evaluating both the full-sample fit of the model and its forecasting performance. Specifically, we evaluate the ability of the MMReDCC model to provide accurate multi-steps-ahead covariance predictions against existing competitors not accounting for time-varying long term dynamics.

6.1. Small sample accuracy comparison

In small dimensional applications, according to Table 1, the QMLE is applicable and represents the most efficient estimator, at least asymptotically. Hence, a simple way to evaluate the in-sample performance of the proposed approach, is to compare the estimates provided by the IMP method to those obtained by maximizing the quasi-likelihood (QL) with respect to the full parameter vector. To this purpose, we fix the cross-sectional dimension equal to ten assets and fit the MMReDCC model to three different datasets. An overview of the data being used is given in the first table in the Appendix. The first dataset comprises the assets used in Bauwens et al. (2016) and includes series of daily realized covariance matrices estimated using five minute intraday returns over the period February 2001 until December 2009 (2242 observations); the second set is made up of some of the most liquid equities of the S&P 500 traded from October 1997 to July 2008 (2524 observations), while the last one consists of an arbitrarily selected subsample of assets from the dataset used in the work of Boudt et al. (2014). The latter contains series of daily realized covariance matrices obtained with the *CholCov* estimator over the period January 2007–December 2012 (1499 trading days)⁶. As already mentioned, the choice of the realized estimator is not an issue as the model can be fitted to any series of realized variance-covariance matrices as long as they are PDS.

As suggested by a referee, the IMP estimator could also be used to provide accurate initial values for direct QML estimation leading to a reduction of the number of iterations needed to reach convergence and, hence, to substantial computational savings. In this spirit we also consider the additional estimator, denoted as IMP(+), obtained by performing one iteration of the one-step QL optimization, taking the IMP estimate as starting point.

Estimation results for the MMReDCC model parameters by the QML, IMP and IMP(+) estimators are collected in Panel A of Table 8. In the three datasets considered, all methods appear to deliver similar estimates. Short term GARCH coefficients tend to be quite homogeneous across assets and generally significant; the same applies to the short term correlation estimates. As for the parameters driving the long term component, it can be noticed that the estimated θ and ω coefficients are regularly lower for the IMP than for the QML method. This is in line with the prevailing negative bias found in the simulation study. Coming to the analysis of the maximized quasi log-likelihood

⁶Our analysis focuses on open-to-close covariance matrices, whereby noisy overnight returns have not been included in the construction of the estimators. We refer to the cited papers for further details.

Table 7: Prediction intervals

The table reports prediction intervals for variances (left panel) and covariances (right panel) of MMRdDCC model across 1000 simulations.

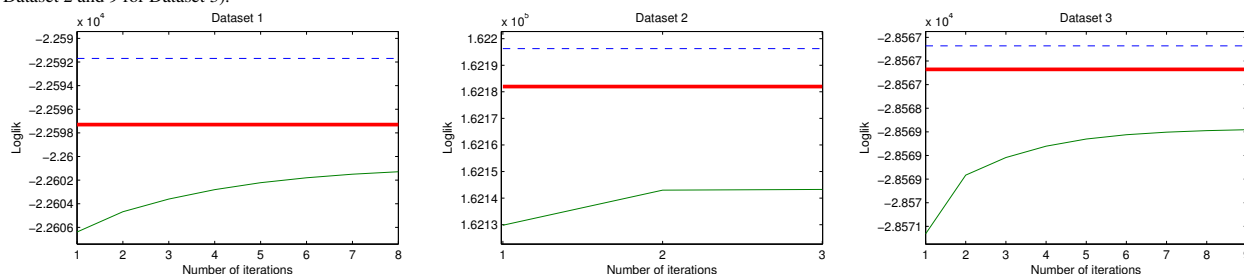
VARIANCES							COVARIANCES							
n	Lead time	T	Nominal coverage	Average coverage	Av.cov. below	Av.cov. above	n	Lead time	T	Nominal coverage	Average coverage	Av.cov. below	Av.cov. above	
5	2	1000	0.90	0.891	0.054	0.054	5	2	1000	0.90	0.897	0.052	0.051	
			0.95	0.945	0.026	0.029				0.95	0.946	0.028	0.026	
			0.99	0.978	0.008	0.014				0.99	0.981	0.007	0.011	
		2000	0.90	0.894	0.053	0.053			2000	0.90	0.906	0.046	0.048	
			0.95	0.951	0.024	0.025				0.95	0.954	0.025	0.021	
			0.99	0.982	0.005	0.012				0.99	0.982	0.007	0.011	
	10	1000	0.90	0.878	0.064	0.059		10	1000	0.90	0.877	0.061	0.062	
			0.95	0.932	0.036	0.032				2000	0.95	0.930	0.035	0.035
			0.99	0.971	0.012	0.017					0.99	0.974	0.010	0.016
		2000	0.90	0.882	0.057	0.061			2000		0.90	0.882	0.060	0.058
			0.95	0.935	0.030	0.034				0.95	0.935	0.035	0.031	
			0.99	0.973	0.009	0.018				0.99	0.978	0.010	0.013	
	20	1000	0.90	0.873	0.062	0.065		20	1000	0.90	0.874	0.065	0.061	
			0.95	0.932	0.033	0.035				2000	0.95	0.930	0.036	0.036
			0.99	0.977	0.006	0.017					0.99	0.973	0.010	0.017
		2000	0.90	0.874	0.067	0.065			2000		0.90	0.879	0.064	0.057
			0.95	0.923	0.035	0.041				2000	0.95	0.933	0.036	0.034
			0.99	0.970	0.008	0.022					0.99	0.971	0.012	0.018
10	2	1000	0.90	0.891	0.053	0.057	10	2	1000		0.90	0.889	0.056	0.055
			0.95	0.940	0.028	0.031				2000	0.95	0.943	0.028	0.029
			0.99	0.979	0.007	0.015					0.99	0.980	0.007	0.013
		2000	0.90	0.895	0.054	0.052			2000		0.90	0.895	0.053	0.053
			0.95	0.948	0.027	0.025				2000	0.95	0.946	0.028	0.027
			0.99	0.983	0.005	0.013					0.99	0.981	0.007	0.012
	10	1000	0.90	0.876	0.060	0.064		10	1000		0.90	0.883	0.060	0.058
			0.95	0.933	0.030	0.037				2000	0.95	0.935	0.032	0.033
			0.99	0.975	0.007	0.018					0.99	0.975	0.010	0.016
		2000	0.90	0.883	0.060	0.057			2000		0.90	0.880	0.058	0.060
			0.95	0.938	0.030	0.030				2000	0.95	0.935	0.032	0.032
			0.99	0.978	0.006	0.014					0.99	0.977	0.009	0.014
	20	1000	0.90	0.873	0.065	0.066		20	1000		0.90	0.873	0.064	0.063
			0.95	0.930	0.033	0.037				2000	0.95	0.932	0.037	0.035
			0.99	0.975	0.007	0.018					0.99	0.973	0.011	0.016
		2000	0.90	0.876	0.060	0.063			2000		0.90	0.870	0.063	0.064
			0.95	0.930	0.033	0.037				2000	0.95	0.934	0.035	0.038
			0.99	0.974	0.008	0.017					0.99	0.972	0.010	0.017
20	2	1000	0.90	0.892	0.049	0.059	20	2	1000		0.90	0.886	0.057	0.057
			0.95	0.943	0.025	0.032				2000	0.95	0.939	0.030	0.031
			0.99	0.981	0.006	0.014					0.99	0.979	0.007	0.013
		2000	0.90	0.892	0.051	0.057			2000		0.90	0.887	0.057	0.056
			0.95	0.946	0.026	0.029				2000	0.95	0.940	0.030	0.030
			0.99	0.983	0.005	0.012					0.99	0.979	0.007	0.013
	10	1000	0.90	0.880	0.055	0.065		10	1000		0.90	0.876	0.062	0.062
			0.95	0.935	0.029	0.036				2000	0.95	0.931	0.034	0.034
			0.99	0.976	0.007	0.017					0.99	0.975	0.009	0.016
		2000	0.90	0.883	0.054	0.063			2000		0.90	0.876	0.061	0.062
			0.95	0.936	0.028	0.036				2000	0.95	0.932	0.034	0.034
			0.99	0.975	0.008	0.017					0.99	0.975	0.009	0.016
	20	1000	0.90	0.877	0.060	0.063		20	1000		0.90	0.873	0.066	0.068
			0.95	0.933	0.032	0.036				2000	0.95	0.930	0.037	0.038
			0.99	0.972	0.009	0.019					0.99	0.970	0.011	0.018
		2000	0.90	0.877	0.059	0.064			2000		0.90	0.875	0.065	0.066
			0.95	0.933	0.033	0.034				2000	0.95	0.931	0.037	0.037
			0.99	0.977	0.007	0.016					0.99	0.972	0.011	0.017
50	2	1000	0.90	0.899	0.045	0.056	50	2	1000		0.90	0.886	0.057	0.057
			0.95	0.950	0.023	0.027				2000	0.95	0.939	0.030	0.030
			0.99	0.985	0.005	0.010					0.99	0.979	0.007	0.013
		2000	0.90	0.897	0.050	0.053			2000		0.90	0.889	0.055	0.056
			0.95	0.948	0.025	0.026				2000	0.95	0.942	0.029	0.029
			0.99	0.985	0.005	0.010					0.99	0.980	0.007	0.013
	10	1000	0.90	0.888	0.051	0.061		10	1000		0.90	0.874	0.063	0.063
			0.95	0.940	0.027	0.033				2000	0.95	0.931	0.034	0.035
			0.99	0.979	0.007	0.015					0.99	0.975	0.009	0.016
		2000	0.90	0.888	0.056	0.057			2000		0.90	0.878	0.061	0.061
			0.95	0.941	0.028	0.030				2000	0.95	0.934	0.033	0.033
			0.99	0.980	0.007	0.013					0.99	0.977	0.008	0.015
	20	1000	0.90	0.879	0.054	0.067		20	1000		0.90	0.864	0.068	0.068
			0.95	0.934	0.029	0.037				2000	0.95	0.923	0.038	0.038
			0.99	0.977	0.007	0.017					0.99	0.971	0.011	0.018
		2000	0.90	0.880	0.057	0.063			2000		0.90	0.868	0.066	0.066
			0.95	0.935	0.031	0.034				2000	0.95	0.926	0.037	0.036
			0.99	0.977	0.007	0.016					0.99	0.973	0.010	0.017

values, it can be seen that, as expected, the QMLE returns the highest QL value for all the datasets, but those obtained by the IMP estimator are very close, and the gap never exceeds 0.04% in relative terms. The IMP(+) further reduces the discrepancy but its contribution is as small as 0.014% on average, thus far from impressive.

The bottom line of Panel A reports test statistics and corresponding p-values of a score test (ST) performed to assess convergence of the IMP and IMP(+) estimators. In practice we test the null hypothesis that $\psi^* = \mathbf{0}$ in the unrestricted model parameterized by $\psi = \hat{\psi}_M + \psi^*$ where $\hat{\psi}_M$ denotes the estimate of ψ obtained by estimation method M . In practice ψ^* can be interpreted as the bias potentially affecting the estimated ψ in case of lack of convergence of the IMP and IMP(+) algorithms. In order to double check our results the test is repeated for the QML estimator. The null is accepted in all cases. This result is confirmed by [figure 2](#) that compares the values of the QL function recorded for the IMP estimator in each iteration (continuous thin line) with the maximum obtained by direct maximization of the QL function (continuous thick line) and by the IMP(+) estimator (dotted line). The plot shows that the IMP algorithm increases the value of the QL function at each step monotonically converging to a value which is very close to the maximum yielded by the direct QML estimator.

Finally, Panel B of Table 8 provides further information on the performance of the estimators measured in terms of mean, standard deviation, first (Q1) and third (Q3) quantiles of the estimated conditional variance, covariance and correlation series. Furthermore, to gain deeper insight on the practical impact that the choice of the estimation algorithm can have on risk management applications, the comparison is extended to the estimated conditional variances of the equally weighted portfolio returns. In general, the distribution of the estimated series do not appear to be very sensitive to the estimation method adopted. The most sizeable differences are observable between QML and IMP(+) estimated conditional variances and covariances of Dataset 3. Nevertheless, the discrepancy becomes negligible if we focus on conditional correlations and, in particular, on portfolio volatility which is the main quantity of interest for risk management applications.

Figure 2: The figure shows the log-likelihood value at the maximum (y-axis) achieved by 1-step QML (dotted line), IMP (continuous thin line) and IMP(+) (continuous thick line), for each of the considered datasets. The number of iterations needed for the IMP optimization to converge is given on the x-axis (8 for Dataset 1, 3 for Dataset 2 and 9 for Dataset 3).



6.2. Forecasting performance

In this subsection we push the analysis to higher dimensions, with the aim of assessing the usefulness of the MMRcDCC model in a forecasting exercise. As benchmarks we consider the consistent RDCC (cRDCC) model of [Bauwens et al. \(2012\)](#) as the closest competitor and a simple Exponentially Weighted Moving Average (EWMA) model. The EWMA predictor appears a natural candidate due to its widespread diffusion among practitioners and in risk management systems like RiskMetrics. If applied to series of daily realized covariance matrices, it is defined by

$$S_t = (1 - \lambda)C_{t-1} + \lambda S_{t-1},$$

where the λ parameter is set equal to the value 0.94 (see also [Golosnoy et al. \(2012\)](#)).

On the other hand, the choice of the cRDCC as a benchmark is supported by two main reasons. First, it assumes that conditional volatilities and correlations mean revert to constant quantities, thus it can be considered as a simplified version of the MMRcDCC model despite not being formally nested in it. Second, the findings of [Boudt et al. \(2014\)](#)

Table 8: Application I. In-sample comparison

Panel A shows parameter estimates with corresponding standard errors in brackets for each of the estimators employed and the three datasets considered (see first table in the Appendix). IMP(+) denotes results achieved after one iteration of the one-step QL optimization, taking the IMP estimate as starting point. The last two rows respectively report the log-likelihood (Loglik) values at the maximum and Score test (ST) statistics with corresponding p-values in brackets. Panel B reports summary statistics for the estimated series of volatilities (Vol), covariances (Cov) and correlations (Corr) across estimators and datasets. The properties of the volatilities (Portf. vol) of the n -dimensional equally weighted portfolios constructed using the estimated conditional covariance matrices are also compared. The number of in-sample observations is 2242 for Dataset 1, 2524 for Dataset 2 and 1499 for Dataset 3.

DATASET 1						DATASET 2						DATASET 3					
PANEL A: PARAMETER ESTIMATES																	
QML		IMP		IMP(+)		QML		IMP		IMP(+)		QML		IMP		IMP(+)	
γ_i	δ_i	γ_i	δ_i	γ_i	δ_i	γ_i	δ_i	γ_i	δ_i	γ_i	δ_i	γ_i	δ_i	γ_i	δ_i	γ_i	δ_i
0.35 (0.10)	0.60 (0.03)	0.34 (0.06)	0.59 (0.03)	0.37 (0.15)	0.55 (0.08)	0.12 (0.04)	0.88 (0.19)	0.10 (0.06)	0.85 (0.10)	0.09 (0.03)	0.82 (0.15)	0.18 (0.07)	0.75 (0.06)	0.18 (0.16)	0.75 (0.07)	0.17 (0.09)	0.75 (0.05)
0.34 (0.38)	0.58 (0.08)	0.31 (0.76)	0.60 (0.05)	0.33 (0.86)	0.58 (0.07)	0.32 (0.15)	0.80 (0.18)	0.33 (0.07)	0.83 (0.12)	0.29 (0.05)	0.82 (0.18)	0.23 (0.20)	0.69 (0.04)	0.23 (0.90)	0.69 (0.05)	0.24 (0.92)	0.68 (0.04)
0.41 (0.04)	0.57 (0.06)	0.40 (0.03)	0.52 (0.05)	0.41 (0.05)	0.51 (0.09)	0.33 (0.08)	0.61 (1.01)	0.28 (0.07)	0.55 (0.10)	0.33 (0.30)	0.52 (0.43)	0.24 (0.04)	0.62 (0.06)	0.25 (0.16)	0.62 (0.21)	0.25 (0.06)	0.61 (0.09)
0.43 (0.06)	0.53 (0.06)	0.38 (0.04)	0.49 (0.06)	0.41 (0.06)	0.48 (0.07)	0.26 (0.03)	0.43 (0.18)	0.24 (0.06)	0.41 (0.01)	0.28 (0.12)	0.38 (0.06)	0.20 (0.05)	0.67 (0.07)	0.19 (0.06)	0.69 (0.07)	0.20 (0.07)	0.68 (0.06)
0.37 (0.05)	0.49 (0.05)	0.37 (0.03)	0.49 (0.04)	0.40 (0.05)	0.48 (0.06)	0.46 (0.08)	0.18 (0.09)	0.49 (0.14)	0.23 (0.05)	0.50 (0.09)	0.22 (0.06)	0.20 (0.06)	0.60 (0.09)	0.21 (0.11)	0.65 (0.12)	0.20 (0.06)	0.59 (0.10)
0.34 (0.05)	0.65 (0.12)	0.32 (0.04)	0.61 (0.06)	0.33 (0.06)	0.60 (0.06)	0.35 (0.14)	0.76 (0.25)	0.34 (0.20)	0.79 (0.28)	0.35 (0.15)	0.78 (0.20)	0.18 (0.11)	0.69 (0.20)	0.18 (0.09)	0.73 (0.13)	0.19 (0.10)	0.68 (0.18)
0.40 (0.05)	0.52 (0.11)	0.42 (0.04)	0.51 (0.05)	0.44 (0.06)	0.49 (0.10)	0.43 (0.09)	0.52 (0.09)	0.23 (0.10)	0.44 (0.62)	0.31 (0.10)	0.36 (0.09)	0.15 (0.09)	0.68 (0.23)	0.14 (0.08)	0.74 (0.19)	0.16 (0.10)	0.66 (0.23)
0.47 (0.04)	0.43 (0.04)	0.45 (0.03)	0.40 (0.05)	0.45 (0.04)	0.40 (0.05)	0.45 (0.21)	0.72 (0.17)	0.43 (0.16)	0.70 (0.01)	0.45 (0.19)	0.68 (0.03)	0.18 (0.07)	0.75 (0.16)	0.18 (0.16)	0.75 (0.40)	0.18 (0.08)	0.75 (0.16)
0.31 (0.06)	0.61 (0.08)	0.31 (0.04)	0.59 (0.05)	0.32 (0.04)	0.57 (0.08)	0.18 (0.06)	0.59 (0.19)	0.16 (0.15)	0.63 (0.04)	0.20 (0.17)	0.60 (0.13)	0.18 (0.10)	0.74 (0.27)	0.17 (0.14)	0.75 (0.23)	0.17 (0.20)	0.74 (0.50)
0.34 (0.06)	0.55 (0.09)	0.31 (0.04)	0.58 (0.06)	0.35 (0.05)	0.56 (0.08)	0.43 (0.11)	0.36 (0.09)	0.47 (0.17)	0.27 (0.01)	0.48 (0.12)	0.28 (0.10)	0.14 (0.04)	0.78 (0.05)	0.14 (0.06)	0.80 (0.10)	0.14 (0.04)	0.78 (0.05)
α	β	α	β	α	β	α	β	α	β	α	β	α	β	α	β	α	β
0.07 (0.02)	0.91 (0.08)	0.08 (0.01)	0.88 (0.06)	0.07 (0.02)	0.88 (0.08)	0.05 (0.01)	0.86 (0.16)	0.04 (0.01)	0.89 (0.10)	0.05 (0.00)	0.87 (0.11)	0.01 (0.00)	0.80 (0.10)	0.01 (0.00)	0.88 (0.05)	0.01 (0.00)	0.77 (0.05)
θ	ω	θ	ω	θ	ω	θ	ω	θ	ω	θ	ω	θ	ω	θ	ω	θ	ω
0.88 (0.01)	4.57 (0.01)	0.83 (0.00)	4.22 (0.01)	0.87 (0.00)	5.69 (0.03)	0.91 (0.21)	3.67 (0.02)	0.88 (0.02)	2.91 (0.07)	0.90 (0.06)	3.46 (0.19)	0.84 (0.02)	5.52 (1.58)	0.81 (0.30)	5.16 (0.57)	0.82 (0.01)	5.56 (0.44)
Loglik		Loglik		Loglik		Loglik		Loglik		Loglik		Loglik		Loglik		Loglik	
-22592		-22601		-22597		162196		162143		162180		-28567		-28568		-28567	
ST		ST		ST		ST		ST		ST		ST		ST		ST	
-0.001 (1.00)		-0.026 (1.00)		-0.001 (1.00)		0.103 (1.00)		0.345 (1.00)		0.290 (1.00)		0.000 (1.00)		0.030 (1.00)		0.001 (1.00)	
PANEL B: PROPERTIES OF ESTIMATED SERIES																	
		QML		IMP		IMP(+)				QML		IMP		IMP(+)			
Vol	mean	2.98	3.06	3.14													
	std	5.70	5.84	5.89													
	Q1	0.70	0.70	0.74													
	Q3	2.60	2.69	2.78													
Cov	mean	1.20	1.24	1.26													
	std	2.45	2.47	2.49													
	Q1	0.20	0.21	0.22													
	Q3	1.03	1.09	1.10													
Corr	mean	0.37	0.39	0.38													
	std	0.10	0.10	0.10													
	Q1	0.30	0.31	0.31													
	Q3	0.44	0.45	0.44													
Portf. vol	mean	0.95	0.97	0.99													
	std	0.69	0.69	0.69													
	Q1	0.52	0.53	0.54													
	Q3	1.10	1.13	1.14													
Vol	mean	17.33	12.83	11.75													
	std	23.93	19.86	18.35													
	Q1	4.38	3.30	3.07													
	Q3	12.19	11.15	10.23													
Cov	mean	7.16	5.20	4.81													
	std	8.94	7.03	6.53													
	Q1	1.85	1.23	1.14													
	Q3	7.17	5.21	4.76													
Corr	mean	0.42	0.42	0.42													
	std	0.08	0.09	0.09													
	Q1	0.36	0.35	0.35													
	Q3	0.48	0.48	0.48													
Portf. vol	mean	2.29	2.10	2.02													
	std	1.40	1.25	1.20													
	Q1	1.47	1.20	1.16													
	Q3	2.63	2.41	2.30													

show that the cRDCC model favorably compares with some widely used competitors, such as the HEAVY (Noureddin et al. (2012)) and the cDCC (Aielli (2013)) model, in forecasting Value-at-Risk. In order to estimate the cRDCC in high dimension, we apply a three stage QML estimation procedure as suggested by Bauwens et al. (2012), where the constant long term covariance matrix is consistently targeted by the unconditional covariance. This drastically reduces the number of parameters to be estimated to $2n + 2$.

The dataset, also used by Laurent et al. (2012), contains realized covariance matrices based on intraday returns computed from 6-minute intervals last mid-quotes of 46 assets traded in the NYSE and NASDAQ over the period January 5, 1999 to November 14, 2008, for a total of 2483 observations.

Table 9 reports parameter estimates obtained by fitting the MMReDCC and cRDCC models over the full sample period. As emerges from Panel A, the MMReDCC outperforms the cRDCC in terms of the AIC and BIC criteria, which are both minimized for the MMReDCC. The univariate GARCH(1,1) parameters $\bar{\gamma}$ and $\bar{\delta}$, reported in averaged values across series, largely agree with each other, while the correlation estimates are slightly different across the two models, with the cRDCC showing a higher level of persistence.

To closely examine the difference in the fit of the models, consider the estimated conditional correlations between two representative pairs of stocks. The first, presented in the upper panel of Figure 3, includes two financial assets: American Express (AXP) and Bank of America (BAC), while the second pair, in the lower panel, includes stocks from different sectors, i.e. McDonald's (MCD) and Wells & Fargo (WFC). In general the correlations returned by the MMReDCC model appear to be characterized by more pronounced fluctuations. At the beginning of the sample the correlation paths from the two models evolve around the same mean level while at the burst of the dot-com bubble in 2002 the MMReDCC correlations appear to be characterized by a positive level shift which is not present in the cRDCC series. For the remainder of the sample the cRDCC correlations are on average lower than those obtained from the MMReDCC. Given the close similarity between the models, this can be reasonably explained by the fact that the parameters θ and ω driving the long term (co)volatilities dynamics of the MMReDCC allow for a higher flexibility of the model and consequently for a better responsiveness of correlations in periods of pronounced market volatility.

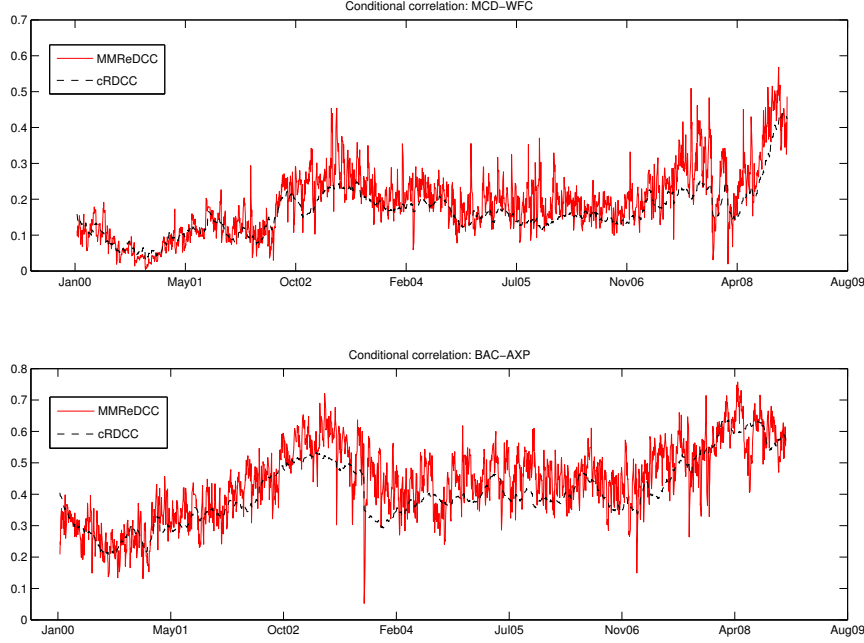
Table 9: **Application II. Full sample estimates and implemented loss functions**

Panel A reports full sample estimates from the MMReDCC and cRDCC model, where $\bar{\gamma}$ and $\bar{\delta}$ are averaged across the n series. AIC and BIC criteria have been rescaled by the number of observations. Panel B contains the loss functions chosen to evaluate the models forecasting ability. S_t denotes the predicted conditional covariance matrix while C_t is the 6-minute realized measure chosen as proxy for the latent covariance matrix.

PANEL A: FULL SAMPLE ESTIMATES		
	MMReDCC	cRDCC
$\bar{\gamma}$	0.381 (0.087)	0.373 (0.180)
$\bar{\delta}$	0.543 (0.110)	0.551 (0.201)
α	0.016 (0.001)	0.020 (0.005)
β	0.950 (0.002)	0.974 (0.007)
θ	0.761 (0.027)	
ω	3.278 (0.785)	
Loglik	787304	683817
AIC	-633	-617
BIC	-630	-616
PANEL B: LOSS FUNCTIONS		
ST	Stein	$\text{tr}(S_t^{-1}C_t) - \log S_t^{-1}C_t - n$
vND	von Neumann Divergence	$\text{tr}(C_t \log C_t - C_t \log S_t - C_t + S_t)$
QLIK	Qlike	$\log S_t + \text{tr}(S_t^{-1}C_t)$

To determine whether the MMReDCC model can lead to gains in forecasting accuracy we compute predictions of the conditional covariance matrix of daily returns at 1, 5, 10 and 20 steps-ahead making use of the bootstrap procedure

Figure 3: Estimated conditional correlation of MCD-WFC (upper panel) and of AXP-BAC (lower panel).



explained in Section 5.⁷ A similar approach is also applied to the cRDCC model, while predictions from the EWMA are obtained analytically, since this model implies that $E(C_{t+h}|\mathfrak{F}_t) = E(C_{t+h-1}|\mathfrak{F}_t)$. To shorten computational time, estimation is performed using a fixed-rolling window scheme with window length equal to 1483 observations that shifts forward every twenty days, over which parameter estimates are kept fixed. The number of re-estimations of each model is equal to fifty, and the out-of-sample evaluation is performed on 1000 trading days.

The forecasting period is characterized by drastic changes in volatility dynamics, as emerges from the summary statistics given in the second table in the Appendix. To better analyze to what extent this impacts on the performance of the models, we break the evaluation sample into two sub-samples. Their differences can be visualized by looking at Figure 4, which shows the realized variance of the equally weighted portfolio made of the 46 assets used in the application. The upper panel spans the period from November, 2004 until end of June, 2007, where the market experiences a situation of stability after the turmoil of the 2000-2003 dot-com bubble. On the other hand, the period from July, 2007 to November, 2008, highlighting a widespread turbulence on the market, coincides with the burst of the subprime financial crisis which reaches its peak with the collapse of Lehman Brothers in September 2008. During the last four months of the latter sub-sample, the unconditional volatility of the portfolio is roughly ten times higher than over the first sub-period.

The comparison of the models forecasting ability is performed using the consistent⁸ loss functions defined in Panel B of Table 9, for which we report averaged values over the two out-of-sample periods considered. The test of [Giacomini and White \(2006\)](#) (GW) is used to examine the relative performance of the MMRReDCC model with respect to the cRDCC and the EWMA. Namely, for each loss function L , the loss differential at time t is denoted as $\delta_t = L(C_{t+h}, S_{t+h|t}^{MMReDCC}) - L(C_{t+h}, S_{t+h|t}^{benchmark})$, where C_t is the the 6-minute realized covariance chosen as proxy for the true matrix. This difference is expected to be zero if neither of the models is superior, otherwise, negative (positive) values correspond to a superior forecasting performance of the MMRReDCC (benchmark). In addition, consistently with the in-sample analysis performed in Section 6.1, we also assess, using the univariate version of the $QLIK$ loss function⁹, the ability of the different models to accurately predict the volatility of an equally weighted

⁷We performed the same exercise using a number of bootstrap replicates equal to 1000, 2000 and 5000, without achieving qualitatively different results. Those we report are for $B = 5000$.

⁸The term *consistent* is used according to [Laurent et al. \(2013\)](#).

⁹As given by [Patton \(2011\)](#), the formula is $QLIK_t = \log(S_{ii,t}) + \frac{C_{ii,t}}{S_{ii,t}}$.

portfolio including all the 46 assets.

The null of equal predictive accuracy is implemented as the following t-statistic

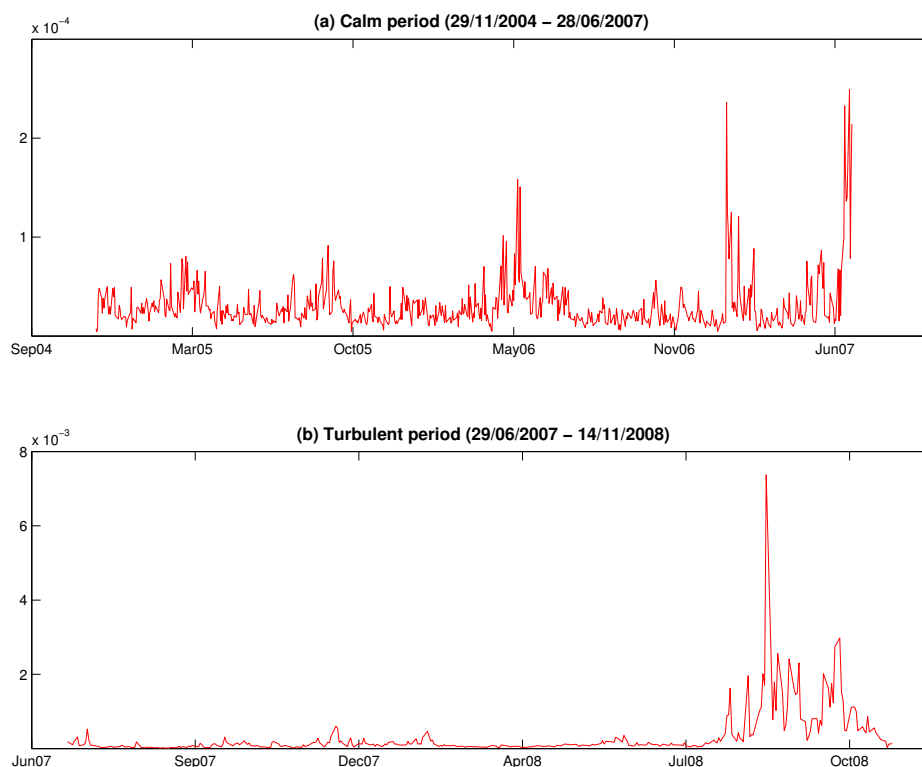
$$GW = \sqrt{T - \tau + h} \frac{\sum_{t=\tau+h}^T \delta_t}{\sqrt{\text{avar}\left(\sum_{t=\tau+h}^T \delta_t\right)}}$$

and the Newey-West estimator is used to consistently estimate the long-run variance of $\sum_{t=\tau+h}^T \delta_t$.

Table 10 shows the resulting average loss differences summarized by horizon. The value achieved by either the EWMA or the cRDCC is in italic if the model is favored by the GW test, in bold if the test favors the MMRdDCC or underlined if the test is indecisive.

Figure 4: Equally weighted portfolio daily realized variance

The figure shows the daily realized variance over the forecasting period of the equally weighted portfolio composed of the 46 assets used in the empirical application and listed in Table A.13. The sample is divided into a more calm period (upper panel, 650 observations) and a more volatile period (lower panel, 350 observations).



According to Panel A, the MMRdDCC model is not leading to particularly impressive gains in forecasting accuracy compared to the two benchmarks. When focusing on direct evaluation of forecasts of the whole RC matrix, the cRDCC is prevailing at the shortest horizon according to all loss functions, while for $h > 1$ they fail to point towards a unique winner as the overall performance of the models is pretty similar and the test is often inconclusive. Despite being the simplest model, the EWMA is found to perform no worse than the other two and to be preferred twice by the vND over the MMRdDCC. Considering that the period covered by Panel A is characterized by a relatively small and slow-moving market volatility, these results are probably not surprising for two reasons. First, it is known that in such circumstances highly parameterized sophisticated models suffer from additional parameter uncertainty, thus being more heavily penalized than model featuring simple parameterizations. Second, when the underlying process exhibits smooth dynamics, it is more complicated for the MMRdDCC model to disentangle the different volatility components, thus suggesting that accurate predictions can be obtained by employing models that do not necessarily account for time-varying long run levels.

As we move to analyze the results in Panel B, the situation is quickly reversed. The cRDCC is still minimizing two out of three loss functions at the one-step horizon, but in all other cases it is evident that, whenever the models predictive abilities can be distinguished, the GW test decides in favor of the MMRReDCC. The over-performance of the MMRReDCC is particularly strong at the 20-day horizon, when it delivers the optimal covariance forecasts according to the whole set of losses.

A slightly different situation arises when we move to the analysis of portfolio volatility forecasts. In this case the forecasting performance of the MMRReDCC model appears to be more stable over time. In period A, at the 1-day horizon the MMRReDCC is outperforming the EWMA and doing not significantly worse than the cRDCC. At longer horizons, it is always prevailing over its competitors, the only exception being represented by the CRDCC, for which at horizon 20 we cannot reject the null of equal predictive ability. In period B, again the worst performance is recorded for the 1-day horizon but, for longer horizons, the MMRReDCC is performing significantly better than its competitors in all cases except for the 10-day horizon when the comparison with the EWMA result is indecisive.

Table 11 offers a closer inspection of the models relative performance by reporting GW test results across univariate (co)volatilities and correlations. For sake of space, only the QLIK case is considered. Each panel of the table records the number of series (out of 1081 (co)volatilities and 1035 correlations) for which the test favors the MMRReDCC, one of the benchmarks or gives no decision. Results are mostly in accordance with those achieved for the whole covariance matrix and stress the evidence that in periods of calm (Panel A) there is almost no benefit from employing the MMRReDCC model for (co)volatility prediction. The gain in terms of correlations is marginal and only achieved with respect to the EWMA. On the other hand, sensibly better results are obtained over the final period (Panel B), both in terms of (co)volatility and correlation dynamics. Noticeably, the number of cases favoring the MMRReDCC increases with h and becomes striking already at $h = 10$.

Overall, the main message we can get from these empirical results is that while constant long-term models may be preferred in moderately volatile time periods, the benefits from the MMRReDCC model can be fully appreciated in periods of market instability. In those cases, the flexibility of the model assures a higher responsiveness and more reliable out-of-sample forecasts.

Table 10: Multi-step-ahead forecast evaluation

The table reports averaged values of the loss functions listed in Table 9. Results are reported across the out-of-sample period divided into a more calm period (Panel A, November 2004 to July 2007) and a more turbulent period (Panel B, July 2007 to November 2008). In the last row of each panel we also report the averaged QLIK of the out-of-sample variance of the equally weighted portfolio obtained using the predicted covariance matrices of the models. For each horizon, we perform pairwise Giacomini-White (GW) tests for the significance at 5% level of the loss difference between the MMRReDCC and each benchmark: the competitor is in italic if it is favored by the test, in bold if the MMRReDCC is favored and underlined if the test is indecisive.

	Horizon 1			Horizon 5			Horizon 10			Horizon 20		
	MMReDCC	EWMA	cReDCC	MMReDCC	EWMA	cReDCC	MMReDCC	EWMA	cReDCC	MMReDCC	EWMA	cReDCC
PANEL A: 29-11-2004/01-07-2007												
ST	37.37	37.52	36.56	38.08	38.62	38.39	38.80	<u>39.24</u>	39.45	39.05	<u>40.01</u>	41.43
vND	0.003	<u>0.003</u>	<i>0.003</i>	0.003	<i>0.003</i>	<u>0.003</u>	0.003	0.003	<u>0.003</u>	0.003	<i>0.003</i>	0.004
QLIK	-386.62	<u>-386.46</u>	<i>-386.43</i>	-385.74	-385.20	-385.43	-385.02	<u>-384.58</u>	-384.38	-383.96	<u>-383.79</u>	-382.38
Portf. vol	-9.69	-9.55	<u>-9.69</u>	-9.75	-9.49	-9.70	-9.789	-9.48	-9.75	-9.83	-9.46	<u>-9.84</u>
PANEL B: 02-07-2007/14-11-2008												
ST	40.12	<u>43.88</u>	39.29	48.03	50.04	<u>49.75</u>	52.76	54.38	58.05	63.08	69.28	72.25
vND	0.023	0.026	0.025	0.030	<u>0.032</u>	0.033	0.043	0.047	0.044	0.045	0.054	0.054
QLIK	-338.75	<u>-338.00</u>	<i>-342.58</i>	-337.35	-332.04	-335.33	-328.48	<u>-327.86</u>	-324.19	-318.29	-312.09	-309.12
Portf. vol	-7.57	-7.43	<i>-7.69</i>	-7.70	-7.41	-7.34	-7.61	<u>-7.37</u>	-6.88	-7.16	-6.72	-5.88

7. Conclusions

The estimation procedure proposed in the paper allows to extend the range of applicability of the MMRReDCC model to large dimensional portfolios such as those encountered in risk management practice. In order to reach this objective, we face two well-known challenges in multivariate time series modeling, namely high-dimensional estimation and multi-step ahead forecasting.

Table 11: GW test results across series

Unconditional Giacomini-White (GW) test results at 5% level of significance using the QLIK function. Each panel of the table records the number of series for which the MMReDCC is favored, for which there is no decision and for which one of the benchmarks is favored. Results are differentiated between conditional (co)volatilities (1081 series) and correlations (1035 series).

(Co)volatilities					Correlations			
PANEL A: 29-11-2004/01-07-2007								
Horizon	Favors MMReDCC	Indecisive	Favors B	Model B	Favors MMReDCC	Indecisive	Favors B	Model B
1	155	732	194	EWMA	62	669	304	EWMA
	24	447	610	cRDCC	87	522	426	cRDCC
5	121	833	127	EWMA	89	882	64	EWMA
	20	369	692	cRDCC	114	427	494	cRDCC
10	33	948	100	EWMA	72	906	57	EWMA
	37	356	688	cRDCC	213	503	319	cRDCC
20	51	850	180	EWMA	118	877	40	EWMA
	77	512	492	cRDCC	108	605	322	cRDCC
PANEL B: 02-07-2007/14-11-2008								
Horizon	Favors MMReDCC	Indecisive	Favors B	Model B	Favors MMReDCC	Indecisive	Favors B	Model B
1	41	853	187	EWMA	130	689	133	EWMA
	5	187	889	cRDCC	266	627	142	cRDCC
5	106	910	65	EWMA	78	911	46	EWMA
	429	620	32	cRDCC	502	505	28	cRDCC
10	198	883	0	EWMA	217	791	27	EWMA
	739	340	2	cRDCC	567	454	14	cRDCC
20	193	888	0	EWMA	339	687	9	EWMA
	835	246	0	cRDCC	626	405	4	cRDCC

To face the former challenge, we implement a feasible estimation procedure, the Iterative Moment based Profiling (IMP) algorithm. It profiles out the parameters of the scale MIDAS intercept matrix and iteratively maximizes the likelihood in terms of the other parameters of interest. Whilst not providing an asymptotic inference theory for this method, we investigate the finite sample properties of the estimator via a simulation study, which demonstrates that the IMP estimator delivers accurate estimates irrespective of the initialization method employed. We also compare the one-step QML and IMP estimators on real data sets of small dimension (ten) and find that not only the two estimators deliver very similar in-sample estimates, but also that the loss of the IMP in terms of likelihood values can be considered as negligible. Another application illustrates the usefulness of the IMP algorithm when the model has to be fitted to high dimensional realized covariance matrices. In this respect, the IMP algorithm is reliable from the computational point of view and easy to implement despite the large number of parameters involved in the MMReDCC model. Given its flexibility, we fairly believe that it could be applied to datasets of larger dimensions.

As regards the second challenge, we develop a bootstrap approach to the generation of multi-step-ahead predictions. In an application to a portfolio of forty-six stocks, we provide compelling evidence that the MMReDCC model is useful for out-of-sample forecasting purposes in periods of pronounced market volatility. If compared with existing multivariate competitors not accounting for time-varying long-term dynamics, the MMReDCC is found to deliver the most accurate predictions especially at long-term horizons, thus indicating the importance of allowing for a more flexible long-run component.

Appendix A. Descriptive statistics

Table A.12: **Descriptive statistics of daily realized variances used in Application I**

The table reports descriptive statistics of daily realized variances of the assets included in Dataset 1, 2 and 3 used in the first empirical application. Mean, maximum, minimum and standard deviation for the assets comprised in Dataset 2 multiplied by 1000.

Symbol	Issue name	Mean	Max.	Min.	Std.dev.	Skewness	Kurtosis
Dataset 1: February, 2001 – December, 2009							
AA	Alcoa	5.458	277.308	0.074	16.811	7.178	72.570
AXP	American Express	5.055	176.478	0.112	11.094	7.529	84.686
BAC	Bank of America	1.934	57.543	0.075	3.362	7.319	85.006
KO	Coca Cola	2.455	43.106	0.084	3.412	4.724	36.234
DD	Du Pont	2.073	115.378	0.126	4.155	13.296	288.066
GE	General Electric	4.944	160.241	0.294	8.935	7.635	92.124
IBM	International Business Machines	4.420	201.879	0.077	9.154	8.536	133.699
JPM	JP Morgan	2.529	63.874	0.163	3.728	6.442	68.505
MSFT	Microsoft	3.196	114.256	0.097	7.114	7.232	75.484
XOM	Exxon Mobil	1.414	56.505	0.039	2.254	9.715	180.206
Dataset 2: May, 1997 – July, 2008							
ABT	Abbott Laboratories	0.383	24.941	0.020	0.859	17.264	397.922
T	AT&T,	0.549	45.804	0.017	1.495	17.145	412.001
FISV	Fiserv	0.783	62.858	0.027	1.559	26.114	999.133
ALL	The Allstate Corporation	0.442	98.076	0.011	2.073	41.512	1934.757
GPC	Genuine Parts Company	0.377	88.800	0.017	1.822	45.217	2180.553
AFL	Aflac Incorporated	0.444	26.705	0.015	1.096	14.110	268.010
AA	Alcoa	0.542	12.377	0.035	0.742	7.331	86.153
GE	General Electric	0.397	36.683	0.013	1.148	20.633	559.319
CTL	CenturyLink	0.447	68.713	0.022	1.881	24.783	775.201
C	Citigroup Inc.	0.624	86.143	0.016	2.131	27.458	1036.670
Dataset 3: January, 2007 – December, 2012							
ACAS	American Capital	8.576	331.786	0.060	20.844	7.226	78.667
AET	Aetna	8.163	771.525	0.109	26.593	17.882	467.969
AFL	Aflac Incorporated	9.113	675.348	0.133	27.345	13.811	284.791
AIG	American International Group	8.799	555.098	0.103	26.382	11.459	185.778
AIZ	Assurant	8.613	325.167	0.101	23.230	7.712	79.082
ALL	The Allstate Corporation	8.213	543.714	0.186	24.593	11.277	189.052
AMP	Ameriprise Financial	7.679	264.761	0.129	17.790	6.098	54.262
AXP	American Express Company	8.076	945.750	0.095	30.571	21.795	618.891
BAC	Bank of America	8.450	332.586	0.130	22.830	8.458	96.824
BBT	BB&T Corporation	9.093	613.826	0.087	28.801	11.267	184.837

Table A.13: Descriptive statistics of daily realized variances used in Application II

The table reports descriptive statistics of daily realized variances of the assets used in the second empirical application, where the forecasting sample, spanning from November 29, 2004 to November 14, 2008, is divided into a calm period (650 observations) and a more turbulent period (350 observations) including the 2008 financial crisis. Mean, maximum, minimum and standard deviation multiplied by 1000.

Stock	Issue name	CALM PERIOD: NOVEMBER 29, 2004 TO JUNE 28, 2007 (650 OBSERVATIONS)						TURBULENT PERIOD: JUNE 29, 2007 TO NOVEMBER 14, 2008 (350 OBSERVATIONS)					
		Mean	Max.	Min.	Std.dev.	Skewness	Kurtosis	Mean	Max.	Min.	Std.dev.	Skewness	Kurtosis
AAPL	Apple	0.311	4.466	0.026	0.300	6.122	68.790	0.857	10.972	0.061	1.255	4.256	26.449
ABT	Abbott	0.104	1.130	0.015	0.081	4.861	47.537	0.323	8.174	0.026	0.569	8.419	106.651
AXP	American Express	0.086	1.093	0.007	0.099	5.780	47.133	1.256	31.221	0.084	2.267	7.830	92.517
BA	The Boeing Comp.	0.115	0.544	0.025	0.077	2.395	10.865	0.514	5.729	0.053	0.779	3.237	15.215
BAC	Bank of America	0.069	1.306	0.012	0.071	9.337	144.620	1.485	27.682	0.028	2.620	4.950	38.832
BMJ	Bristol-Myers Squibb Comp.	0.127	2.026	0.018	0.129	7.536	90.933	0.425	8.793	0.024	0.661	6.871	77.031
BP	BP b.l.c.	0.075	0.387	0.014	0.044	2.497	13.212	0.390	6.578	0.022	0.662	4.219	28.954
C	Citigroup Inc.	0.083	1.285	0.012	0.086	6.696	72.308	2.126	101.576	0.052	6.411	11.733	171.657
CAT	Caterpillar	0.160	1.147	0.030	0.123	3.299	19.873	0.680	11.871	0.057	1.131	4.510	33.690
CL	Colgate-Palmolive	0.080	1.180	0.012	0.069	8.110	112.974	0.263	8.921	0.024	0.566	10.735	157.983
CSCO	Cisco Systems	0.155	1.178	0.019	0.101	3.351	24.940	0.617	11.433	0.048	0.941	5.847	55.795
CVX	Chevron Corp.	0.167	1.457	0.029	0.134	3.629	24.839	0.620	16.630	0.015	1.259	7.438	82.373
DELL	Dell	0.175	1.419	0.024	0.129	2.959	19.761	0.732	14.332	0.065	1.203	6.060	55.915
DIS	Walt Disney	0.101	0.792	0.020	0.071	3.980	30.703	0.508	11.824	0.045	0.941	6.206	63.877
EK		0.141	2.230	0.018	0.162	6.454	63.041	0.675	13.468	0.057	1.135	5.379	50.398
EXC	Exelon	0.284	2.442	0.040	0.229	4.005	29.078	2.784	198.169	0.094	11.678	13.995	227.357
F	Ford Motor	0.130	0.911	0.008	0.094	2.953	16.966	0.526	7.137	0.023	0.710	4.055	27.840
FDX	FedEX Corp.	0.066	0.394	0.013	0.044	2.985	16.741	0.678	9.778	0.029	1.345	4.107	23.102
GE	General Electric	0.130	0.698	0.018	0.085	2.409	11.870	0.798	16.042	0.050	1.164	7.451	87.972
GM	General Motors	0.066	0.658	0.010	0.059	4.374	32.912	0.230	3.996	0.021	0.366	4.784	38.162
HD	The Home Depot	0.130	1.066	0.017	0.100	4.439	34.441	0.568	13.935	0.054	1.076	6.738	72.580
HNZ	HNZ Group	0.079	0.469	0.013	0.055	2.968	15.717	0.449	8.579	0.049	0.750	5.163	44.840
HON	Honeywell	0.154	0.774	0.033	0.084	1.948	9.827	0.583	7.633	0.048	0.739	4.109	29.591
IBM	International Business Machines	0.049	0.268	0.006	0.033	2.207	10.479	0.203	5.937	0.009	0.453	7.067	77.765
INTC	Intel Corp.	0.094	0.660	0.014	0.080	3.586	20.288	1.457	23.401	0.033	2.511	4.987	34.377
JNJ	Johnson & Johnson	0.058	0.487	0.008	0.037	3.822	34.657	0.287	10.144	0.019	0.654	10.345	149.370
JPM	JP Morgan	0.096	0.904	0.014	0.065	4.909	49.496	0.347	8.988	0.027	0.645	7.801	95.111
KO	Coca Cola	0.114	0.812	0.020	0.082	2.968	17.734	0.372	14.811	0.027	0.881	12.896	207.667
LLY	Eli Lilly and Co.	0.088	0.823	0.010	0.070	5.304	47.783	0.384	6.073	0.029	0.638	4.163	26.846
MCD	Mc'Donald	0.145	3.978	0.014	0.237	10.523	141.551	0.540	15.346	0.053	1.058	8.788	113.572
MMM	3M Company	0.174	2.270	0.035	0.190	5.990	52.372	4.234	183.609	0.121	15.669	8.439	83.003
MOT	Motorola	0.089	0.463	0.018	0.055	2.370	11.641	0.455	4.675	0.038	0.630	3.455	17.317
MRK	Merck & Co.	0.181	1.471	0.037	0.113	3.865	35.710	0.572	6.101	0.066	0.802	3.863	20.968
MS	Morgan Stanley	0.061	0.449	0.012	0.041	3.540	24.988	0.290	13.867	0.017	0.822	13.206	214.239
MSFT	Microsoft	0.109	1.980	0.015	0.105	9.948	160.134	0.356	6.396	0.031	0.569	4.916	41.259
SLB	Schlumberger Limited	0.068	0.677	0.008	0.053	4.616	38.780	0.277	12.353	0.020	0.757	12.064	186.892
T	AT&T	0.270	2.236	0.042	0.181	3.769	31.499	0.758	19.677	0.065	1.394	8.423	103.219
TWX	Time Warner	0.302	1.371	0.021	0.190	2.005	9.043	1.042	16.600	0.049	1.523	4.660	36.852
UN	Unilever	0.102	0.954	0.012	0.082	4.197	31.853	0.593	15.642	0.028	1.122	7.847	95.793
VZ	Verizon Communications	0.118	4.846	0.024	0.202	20.058	463.740	0.633	11.438	0.032	1.065	4.688	36.505
ORCL	Oracle Corp.	0.051	0.432	0.009	0.036	3.498	26.050	0.233	4.149	0.022	0.369	4.810	40.616
PEP	Pepsico	0.095	0.889	0.017	0.077	4.104	30.453	0.513	13.320	0.015	0.941	8.068	100.758
PFE	Pfizer Inc.	0.068	0.742	0.007	0.063	4.841	38.013	1.356	20.939	0.057	2.009	4.421	32.569
PG	Procter & Gamble	0.091	0.769	0.013	0.062	4.153	36.416	0.370	9.227	0.023	0.631	8.817	114.702
QCOM	Qualcomm	0.141	1.178	0.025	0.111	4.154	30.987	0.551	18.835	0.033	1.256	9.802	132.780
WFC	Well Fargo & Co.	0.177	4.452	0.024	0.211	13.722	263.426	0.632	18.226	0.065	1.201	9.647	134.130

References

- Aielli, G. P., 2013. Dynamic conditional correlation: On properties and estimation. *Journal of Business & Economic Statistics* 31, 282–299.
- Andersen, T., Bollerslev, T., Diebold, F., Ebens, H., 2001. The distribution of realized stock return volatility. *Journal of Financial Economics* 61, 43–76.
- Barndorff-Nielsen, O., Shephard, N., 2001. Normal modified stable processes. *Theory of Probability and Mathematics Statistics* 65, 1–19.
- Barndorff-Nielsen, O. E., Hansen, P. R., Lunde, A., Shephard, N., 2011. Multivariate realised kernels: consistent positive semi-definite estimators of the covariation of equity prices with noise and non-synchronous trading. *Journal of Econometrics* 162 (2), 149–169.
- Bauwens, L., Braione, M., Storti, G., 2016. Forecasting comparison of long term component dynamic models for realized covariance matrices. *Annals of Economics and Statistics*, (Forthcoming).
- Bauwens, L., Hafner, C. M., Pierret, D., 2013. Multivariate volatility modeling of electricity futures. *Journal of Applied Econometrics* 28 (5), 743–761.
- Bauwens, L., Storti, G., Violante, F., 2012. Dynamic conditional correlation models for realized covariance matrices, CORE DP 2012/60.
- Bollerslev, T., 1990. Modeling the coherence in short-run nominal exchange rates: A multivariate generalized ARCH model. *Review of Economics and Statistics* 72, 498–505.
- Boswijk, H. P., 1995. Identifiability of cointegrated systems. Tinbergen Institute Working Paper (95/78).
- Boudt, K., Laurent, S., Lunde, A., Quaadvlieg, R., 2014. Positive semidefinite integrated covariance estimation, factorizations and asynchronicity. *Factorizations and Asynchronicity* (October 8, 2014).
- Chiriac, R., Voev, V., 2011. Modelling and forecasting multivariate realized volatility. *Journal of Applied Econometrics* 26, 922–947.
- Clements, M. P., Smith, J., 1997. The performance of alternative forecasting methods for SETAR models. *International Journal of Forecasting* 13, 463–475.
- Cubadda, G., Guardabascio, B., Hecq, A., 2015. A vector heterogeneous autoregressive index model for realized volatility measures. Tech. rep.
- Engle, R., 2002. Dynamic conditional correlation: A simple class of multivariate generalized autoregressive conditional heteroskedasticity models. *Journal of Business & Economic Statistics* 20 (3), 339–350.
- Engle, R., Kelly, B., 2012. Dynamic equicorrelation. *Journal of Business & Economic Statistics* 30, 212–228.
- Engle, R. F., 2009. High dimension dynamic correlations. *The Methodology and Practice of Econometrics: A Festschrift in Honour of David F. Hendry: A Festschrift in Honour of David F. Hendry*, 122.
- Engle, R. F., Ghysels, E., Sohn, B., 2013. Stock market volatility and macroeconomic fundamentals. *Review of Economics and Statistics* 95 (3), 776–797.
- Engle, R. F., Shephard, N., Sheppard, K., 2008. Fitting vast dimensional time-varying covariance models.
- Fresoli, D. E., Ruiz, E., 2015. The uncertainty of conditional returns, volatilities and correlations in DCC models. *Computational Statistics & Data Analysis*.
- Ghysels, E., Sinko, A., Valkanov, R., 2007. Midas regressions: Further results and new directions. *Econometric Reviews* 26 (1), 53–90.
- Giacomini, R., White, H., 2006. Tests of conditional predictive ability. *Econometrica* 74 (6), 1545–1578.
- Golosnoy, V., Gribisch, B., Liesenfeld, R., 2012. The conditional autoregressive Wishart model for multivariate stock market volatility. *Journal of Econometrics* 167 (1), 211–223.
- Gouriéroux, C., Jasiak, J., Sufana, R., 2009. The Wishart autoregressive process of multivariate stochastic volatility. *Journal of Econometrics* 150, 167–181.
- Hautsch, N., Kyj, L. M., Malec, P., 2015. Do high-frequency data improve high-dimensional portfolio allocations? *Journal of Applied Econometrics* 30 (2), 263–290.
- Jin, X., Maheu, J. M., 2013. Modeling realized covariances and returns. *Journal of Financial Econometrics* 11 (2), 335–369.
- Laurent, S., Rombouts, J. V., Violante, F., 2012. On the forecasting accuracy of multivariate GARCH models. *Journal of Applied Econometrics* 27 (6), 934–955.
- Laurent, S., Rombouts, J. V., Violante, F., 2013. On loss functions and ranking forecasting performances of multivariate volatility models. *Journal of Econometrics* 173 (1), 1–10.
- Morgan, J., 1994. *Introduction to Riskmetrics*. New York: JP Morgan.
- Noureldin, D., Shephard, N., Sheppard, K., 2012. Multivariate high-frequency-based volatility (HEAVY) models. *Journal of Applied Econometrics* 27 (6), 907–933.
- Pascual, L., Romo, J., Ruiz, E., 2006. Bootstrap prediction for returns and volatilities in GARCH models. *Computational Statistics & Data Analysis* 50 (9), 2293–2312.
- Patton, A. J., 2011. Volatility forecast comparison using imperfect volatility proxies. *Journal of Econometrics* 160 (1), 246–256.
- Pedersen, R. S., Rahbek, A., 2014. Multivariate variance targeting in the BEKK–GARCH model. *The Econometrics Journal* 17 (1), 24–55.
- Shephard, N., Sheppard, K. K., 2010. Realising the future: forecasting with high-frequency-based volatility (HEAVY) models. *Journal of Applied Econometrics* 25, 197–231.